Mueller Navelet jets at LHC:
An observable to reveal high energy resummation effects?

Bertrand Ducloué

Laboratoire de Physique Théorique d'Orsay

Paris, May 20th 2013

in collaboration with
L. Szymanowski (NCBJ Warsaw), S. Wallon (UPMC & LPT Orsay)

D. Colferai; F. Schwennsen, L. Szymanowski, S. Wallon, JHEP 1012:026 (2010) 1-72 [arXiv:1002.1365]

B.D., L. Szymanowski, S. Wallon, arXiv:1208.6111

B.D., L. Szymanowski, S. Wallon, arXiv:1302.7012 (to appear in JHEP)

- One of the important longstanding theoretical questions raised by QCD is its behaviour in the perturbative Regge limit $s \gg -t$
- Based on theoretical grounds, one should identify and test suitable observables in order to test this peculiar dynamics

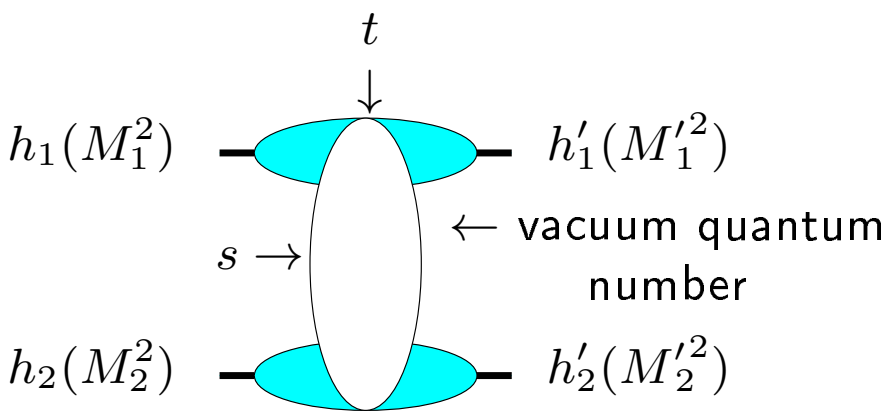

hard scales: $M_1^2,\ M_2^2 \gg \Lambda_{QCD}^2$ or $M_1'^2,\ M_2'^2 \gg \Lambda_{QCD}^2$ or $t \gg \Lambda_{QCD}^2$
where the $t-$channel exchanged state is the so-called hard Pomeron

The different regimes of QCD

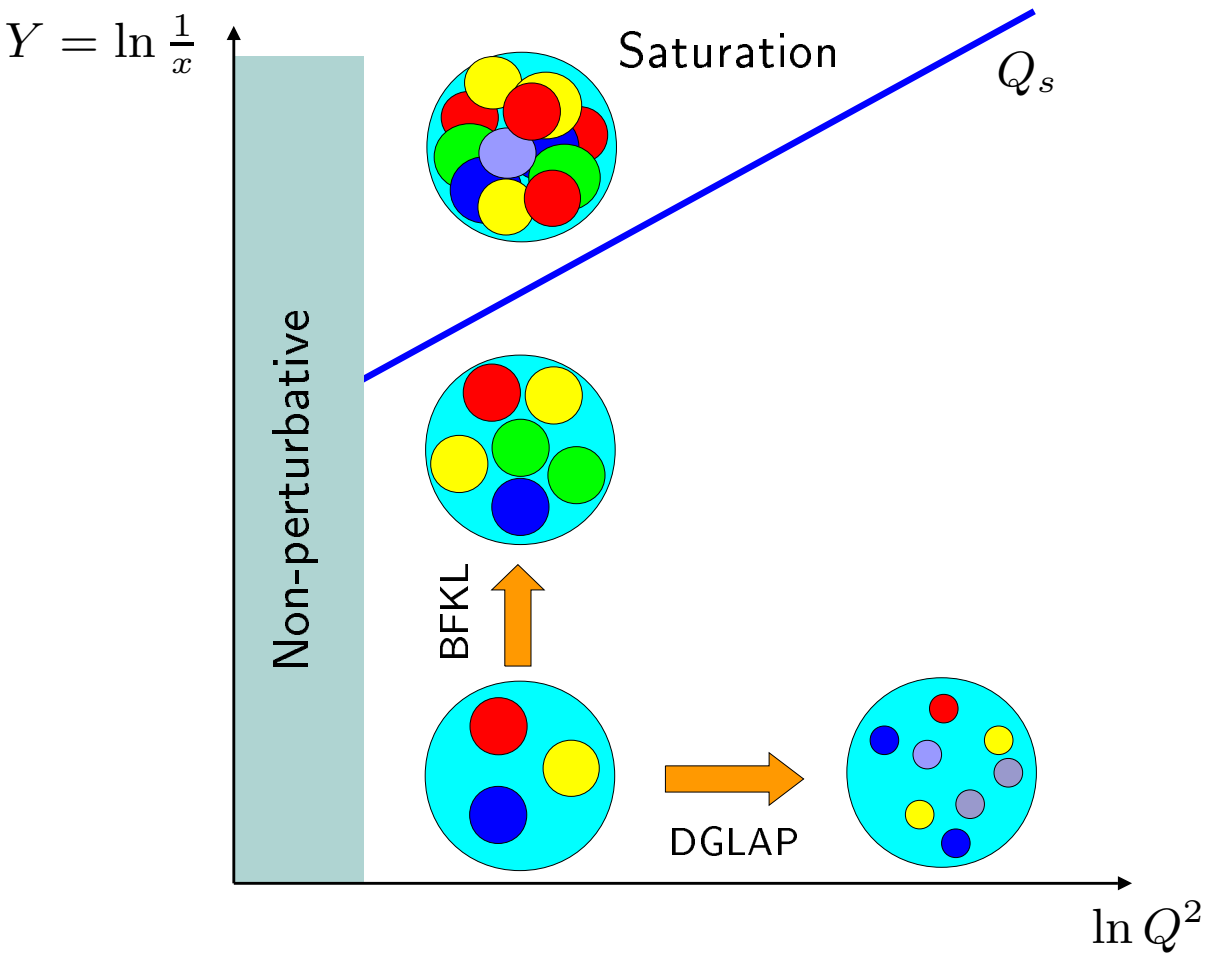

Resummation in QCD: DGLAP vs BFKL

Small values of α_S (perturbation theory applies due to hard scales) can be compensated by large logarithmic enhancements.
$\Rightarrow$ resummation of $\sum_n (\alpha_S \ln A)^n$ series

DGLAP	BFKL
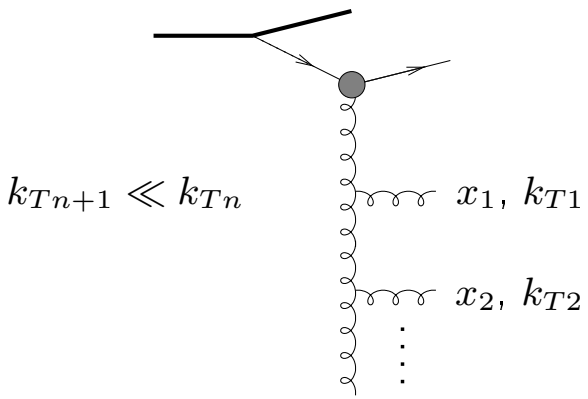	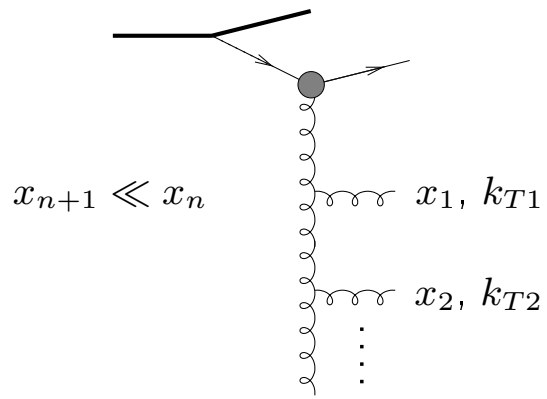
strong ordering in k_T	strong ordering in x
$\sum(\alpha_S \ln \frac{Q^2}{\mu^2})^n$	$\sum(\alpha_S \ln \frac{s}{s_0})^n$

When $\sqrt{s}$ becomes very large, it is expected that a BFKL description is needed to get accurate predictions

How to test QCD in the perturbative Regge limit?

What kind of observables?

- perturbation theory should be applicable:
  selecting external or internal probes with transverse sizes $\ll 1/\Lambda_{QCD}$ or by choosing large t in order to provide the hard scale

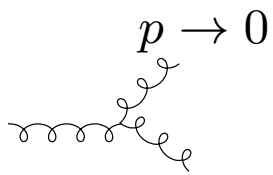

- governed by the *soft* perturbative dynamics of QCD

and *not* by its *collinear* dynamics

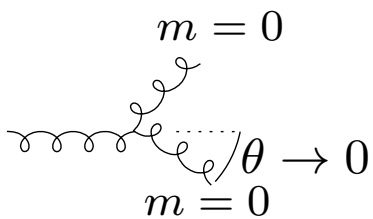

$\Rightarrow$ select semi-hard processes with $s \gg p_{T\,i}^2 \gg \Lambda_{QCD}^2$ where $p_{T\,i}^2$ are typical transverse scale, all of the same order

QCD in the perturbative Regge limit

The amplitude can be written as:

$\mathcal{A} =$ 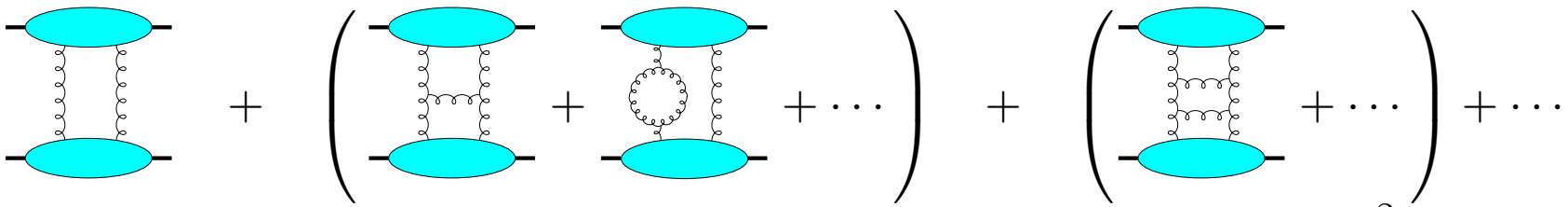 $+ \cdots$

$\sim s$ $\qquad$ $\sim s\,(\alpha_s \ln s)$ $\qquad$ $\sim s\,(\alpha_s \ln s)^2$

this can be put in the following form :

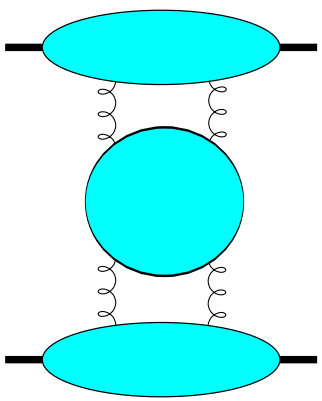

$\leftarrow$ Impact factor

$\leftarrow$ Green's function

$\leftarrow$ Impact factor

Higher order corrections

- Higher order corrections to BFKL kernel are known at NLL order (Lipatov Fadin; Camici, Ciafaloni), now for arbitrary impact parameter
  $\alpha_S \sum_n (\alpha_S \ln s)^n$ resummation

- impact factors are known in some cases at NLL
  - $\gamma^* \to \gamma^*$ at $t = 0$ (Bartels, Colferai, Gieseke, Kyrieleis, Qiao; Balitski, Chirilli)
  - forward jet production (Bartels, Colferai, Vacca)
  - inclusive production of a pair of hadrons separated by a large interval of rapidity (Ivanov, Papa)
  - $\gamma_L^* \to \rho_L$ in the forward limit (Ivanov, Kotsky, Papa)

Mueller-Navelet jets

- Consider two jets (hadrons flying within a narrow cone) separated by a large rapidity, i.e. each of them almost fly in the direction of the hadron "close" to it, and with very similar transverse momenta
- in a pure LO collinear treatment, these two jets should be emitted back to back at leading order: $\Delta\phi - \pi = 0$ ($\Delta\phi = \phi_1 - \phi_2 =$ relative azimuthal angle) and $k_{\perp 1}$=$k_{\perp 2}$. There is no phase space for (untagged) emission between them

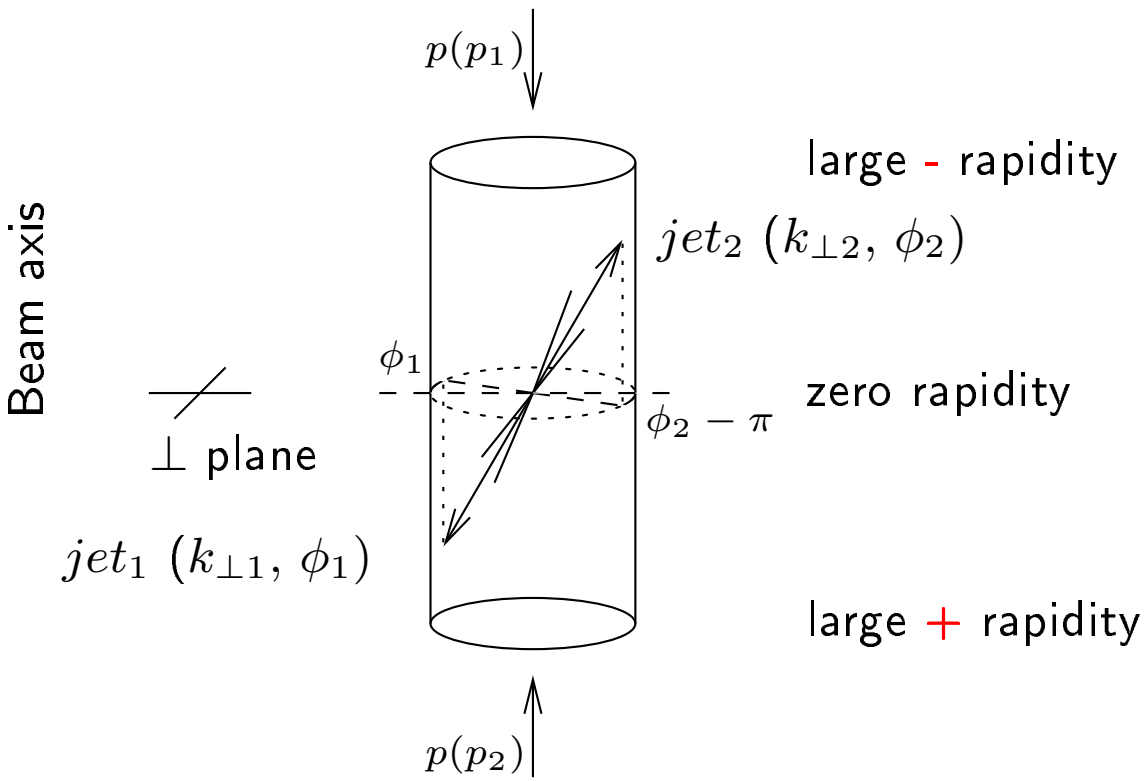

k_T-factorized differential cross-section

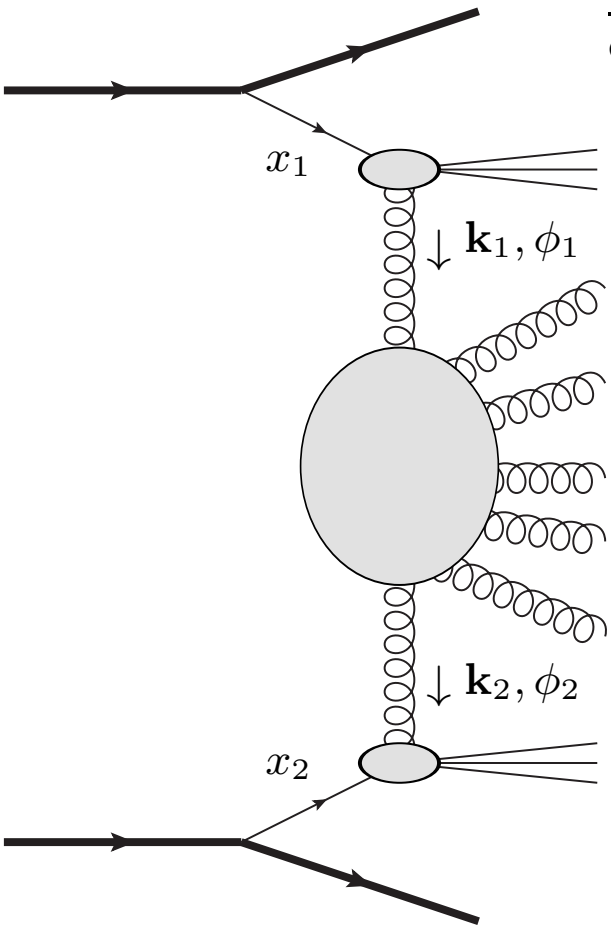

$$\frac{\mathrm{d}\sigma}{\mathrm{d}|\mathbf{k}_{J1}|\,\mathrm{d}|\mathbf{k}_{J2}|\,\mathrm{d}y_{J1}\,\mathrm{d}y_{J2}} = \int \mathrm{d}\phi_{J1}\,\mathrm{d}\phi_{J2} \int \mathrm{d}^2\mathbf{k}_1\,\mathrm{d}^2\mathbf{k}_2$$

$$\times \Phi(\mathbf{k}_{J1}, x_{J1}, -\mathbf{k}_1)$$

$$\times G(\mathbf{k}_1, \mathbf{k}_2, \hat{s})$$

$$\times \Phi(\mathbf{k}_{J2}, x_{J2}, \mathbf{k}_2)$$

with $\Phi(\mathbf{k}_{J2}, x_{J2}, \mathbf{k}_2) = \int \mathrm{d}x_2\, f(x_2) V(\mathbf{k}_2, x_2)$ $\quad f \equiv$ PDF $\quad x_J = \frac{|\mathbf{k}_J|}{\sqrt{s}} e^{y_J}$

- in LL BFKL ($\sim \sum (\alpha_s \ln s)^n$), the emission between these jets leads to a strong decorrelation between the jets, incompatible with $p\bar{p}$ Tevatron collider data

- up to recently, the subseries $\alpha_s \sum (\alpha_s \ln s)^n$ NLL was included only in the Green's function, and not inside the jet vertices
  Sabio Vera, Schwennsen
  Marquet, Royon

- the importance of these corrections was not known

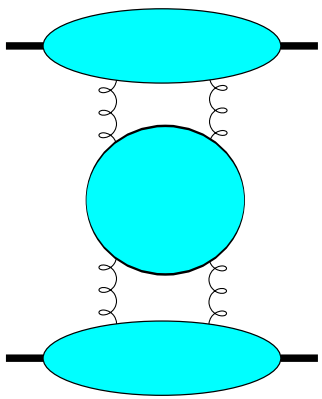

Results for a symmetric configuration

In the following we show results for

- $35\,\mathrm{GeV} < |\mathbf{k}_{J1}|\,, |\mathbf{k}_{J2}| < 60\,\mathrm{GeV}$
- $0 < y_1\,, y_2 < 4.7$

These cuts allow us to compare our predictions with recent results presented by CMS at DIS 2013 (CMS-PAS-FSQ-12-002)

note: unlike experiments we have to set an upper cut on $|\mathbf{k}_{J1}|$ and $|\mathbf{k}_{J2}|$. We have checked that varying this cut doesn't modify our results significantly.

Cross-section

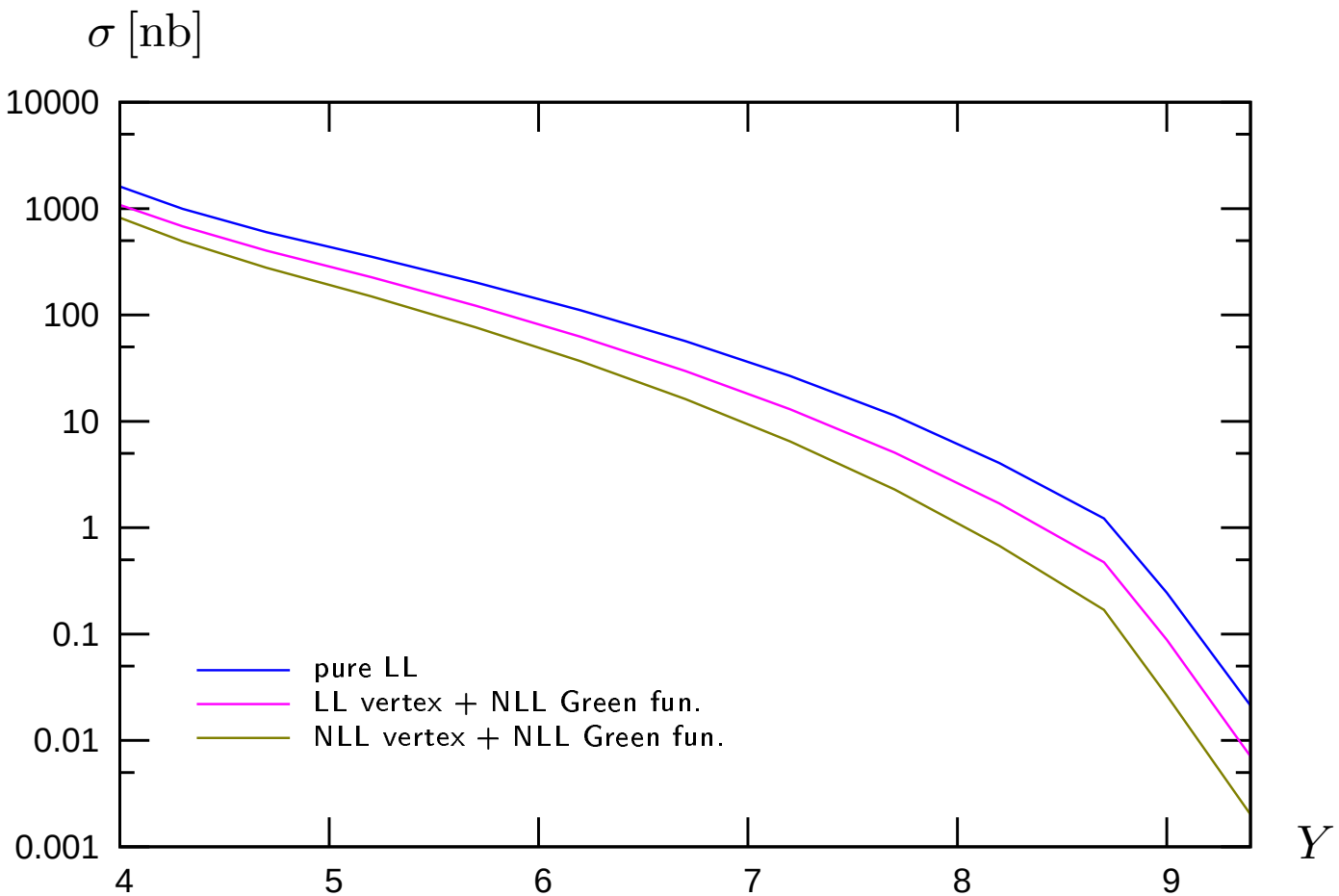

$35\,\mathrm{GeV} < |\mathbf{k}_{J1}| < 60\,\mathrm{GeV}$

$35\,\mathrm{GeV} < |\mathbf{k}_{J2}| < 60\,\mathrm{GeV}$

$0 < y_1 < 4.7$

$0 < y_2 < 4.7$

The effect due to NLL corrections to the jet vertex is of the same order of magnitude as the effect due to NLL corrections to the Green's function.

Cross-section: stability with respect to s_0 and $\mu_R = \mu_F$ changes

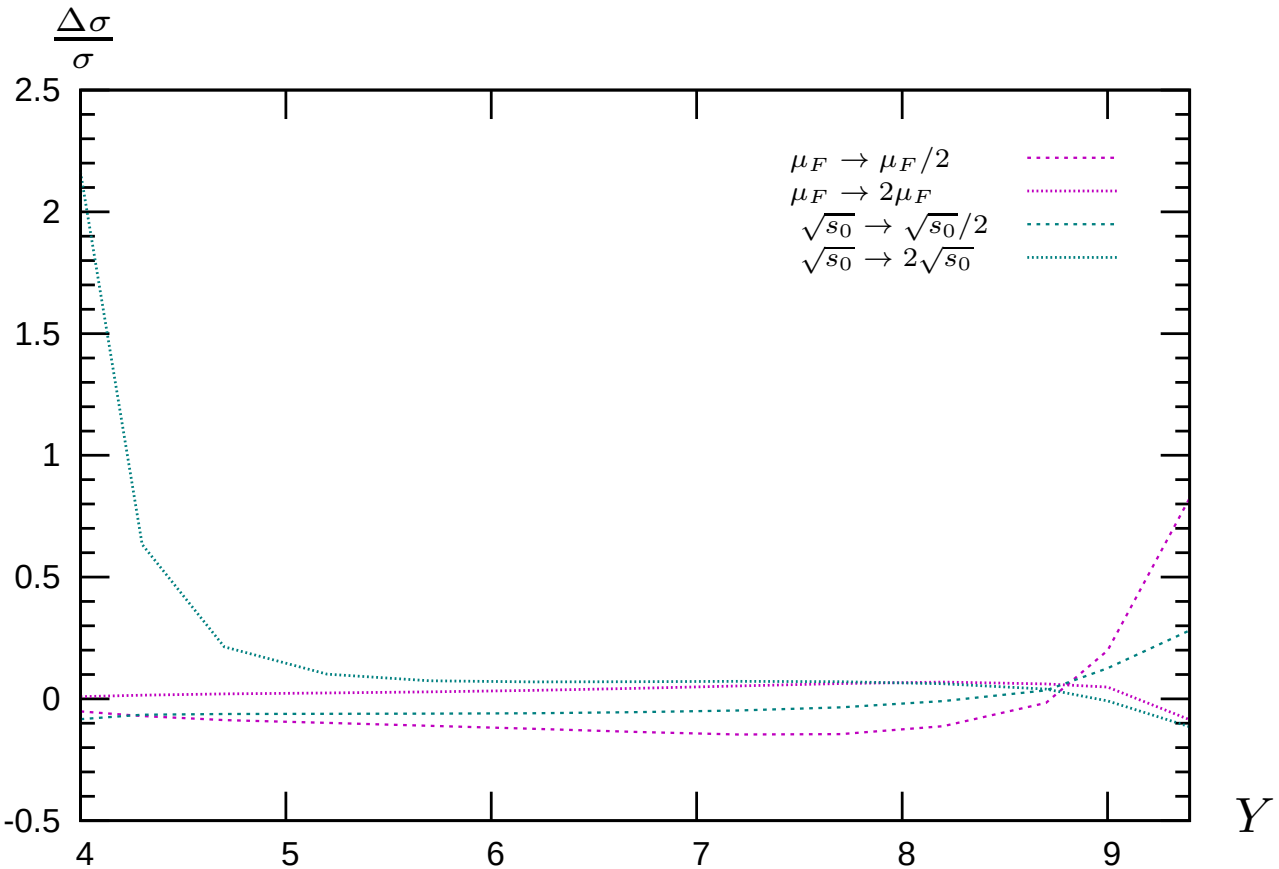

$35\,\mathrm{GeV} < |\mathbf{k}_{J1}| < 60\,\mathrm{GeV}$

$35\,\mathrm{GeV} < |\mathbf{k}_{J2}| < 60\,\mathrm{GeV}$

$0 < y_1 < 4.7$

$0 < y_2 < 4.7$

Our result is rather stable w.r.t s_0 and μ choices for $5 < Y < 9$.

Relative variation of the cross section when using other PDF sets than MSTW 2008

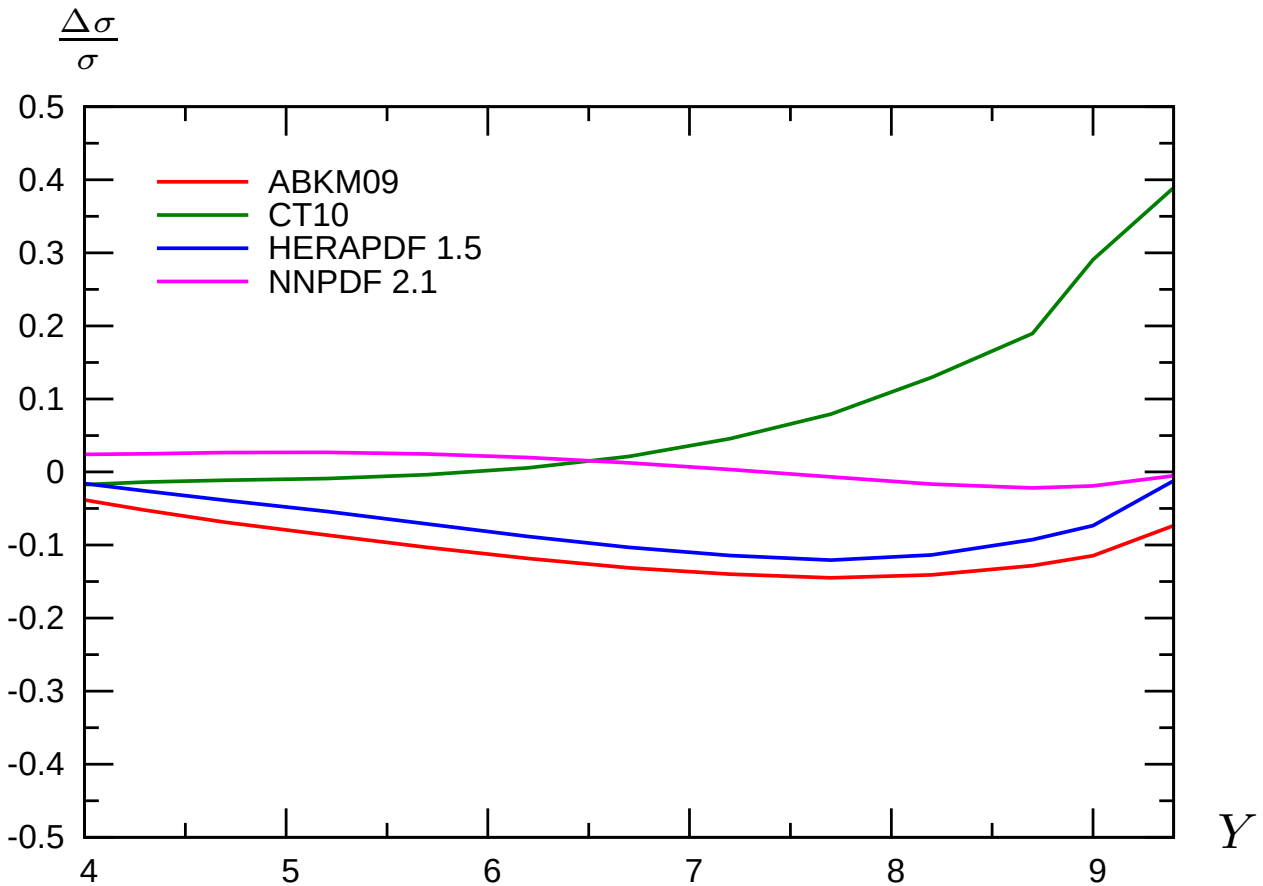

$35\,\mathrm{GeV} < |\mathbf{k}_{J1}| < 60\,\mathrm{GeV}$

$35\,\mathrm{GeV} < |\mathbf{k}_{J2}| < 60\,\mathrm{GeV}$

$0 < y_1 < 4.7$

$0 < y_2 < 4.7$

Azimuthal correlation $\langle \cos\varphi \rangle$

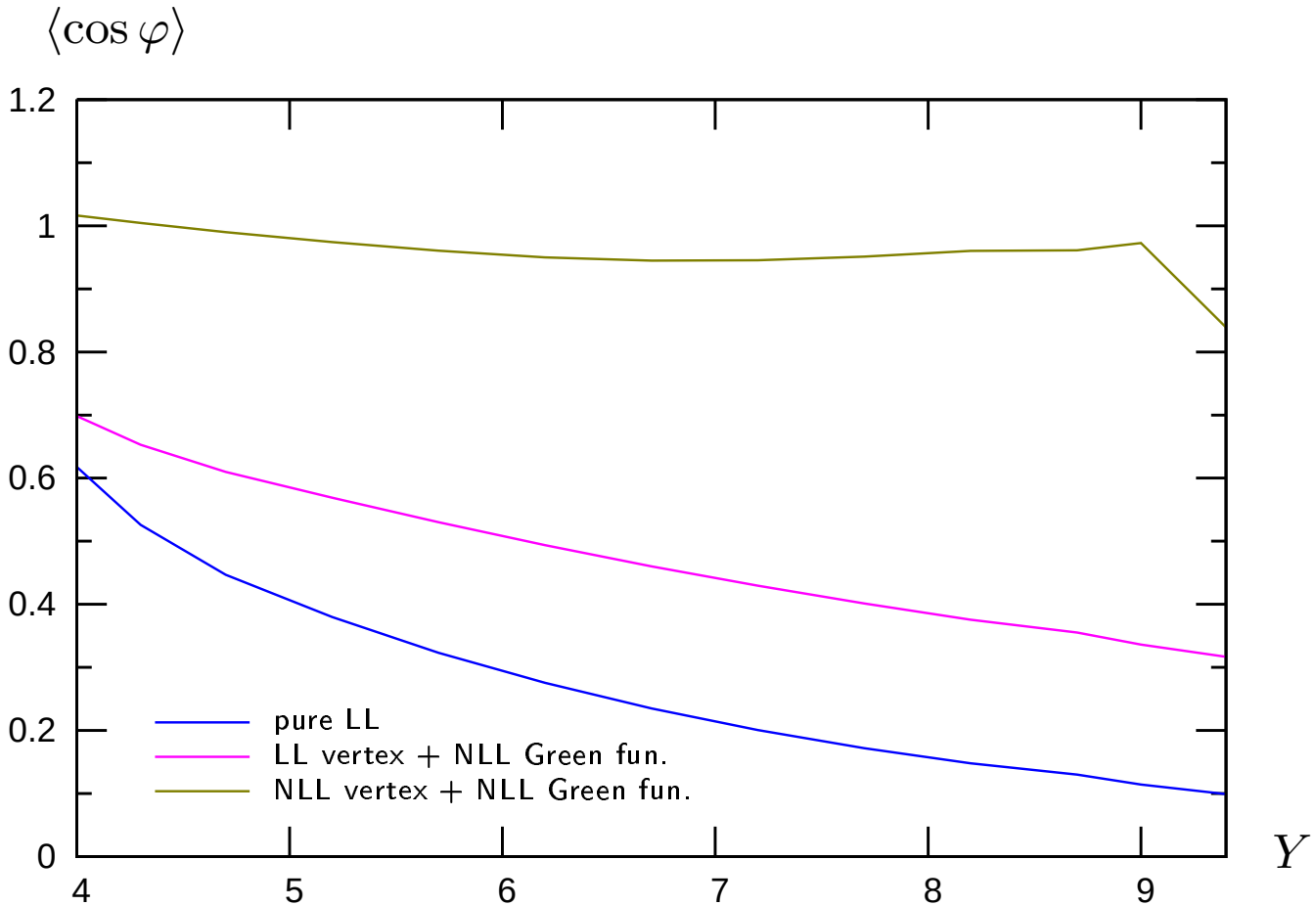

$35\,\mathrm{GeV} < |\mathbf{k}_{J1}| < 60\,\mathrm{GeV}$

$35\,\mathrm{GeV} < |\mathbf{k}_{J2}| < 60\,\mathrm{GeV}$

$0 < y_1 < 4.7$

$0 < y_2 < 4.7$

- The effect of NLL corrections to the jet vertex is very important
- At full NLL accuracy, $\langle \cos\varphi \rangle$ is very flat in Y and very close to 1.

Azimuthal correlation $\langle \cos \varphi \rangle$

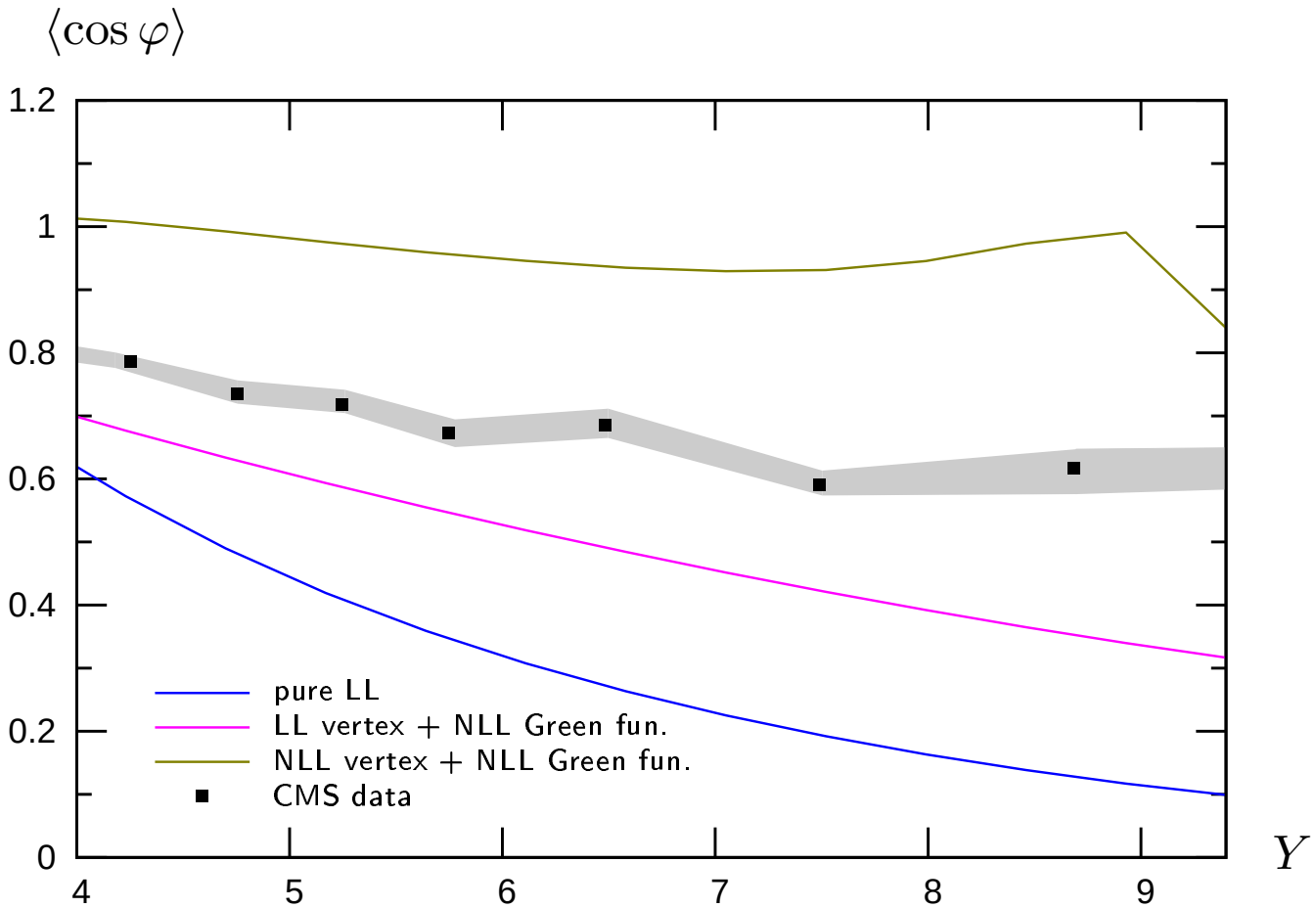

$35\,\mathrm{GeV} < |\mathbf{k}_{J1}| < 60\,\mathrm{GeV}$

$35\,\mathrm{GeV} < |\mathbf{k}_{J2}| < 60\,\mathrm{GeV}$

$0 < y_1 < 4.7$

$0 < y_2 < 4.7$

- None of the BFKL computations describe the data very well

Azimuthal correlation $\langle \cos\varphi \rangle$

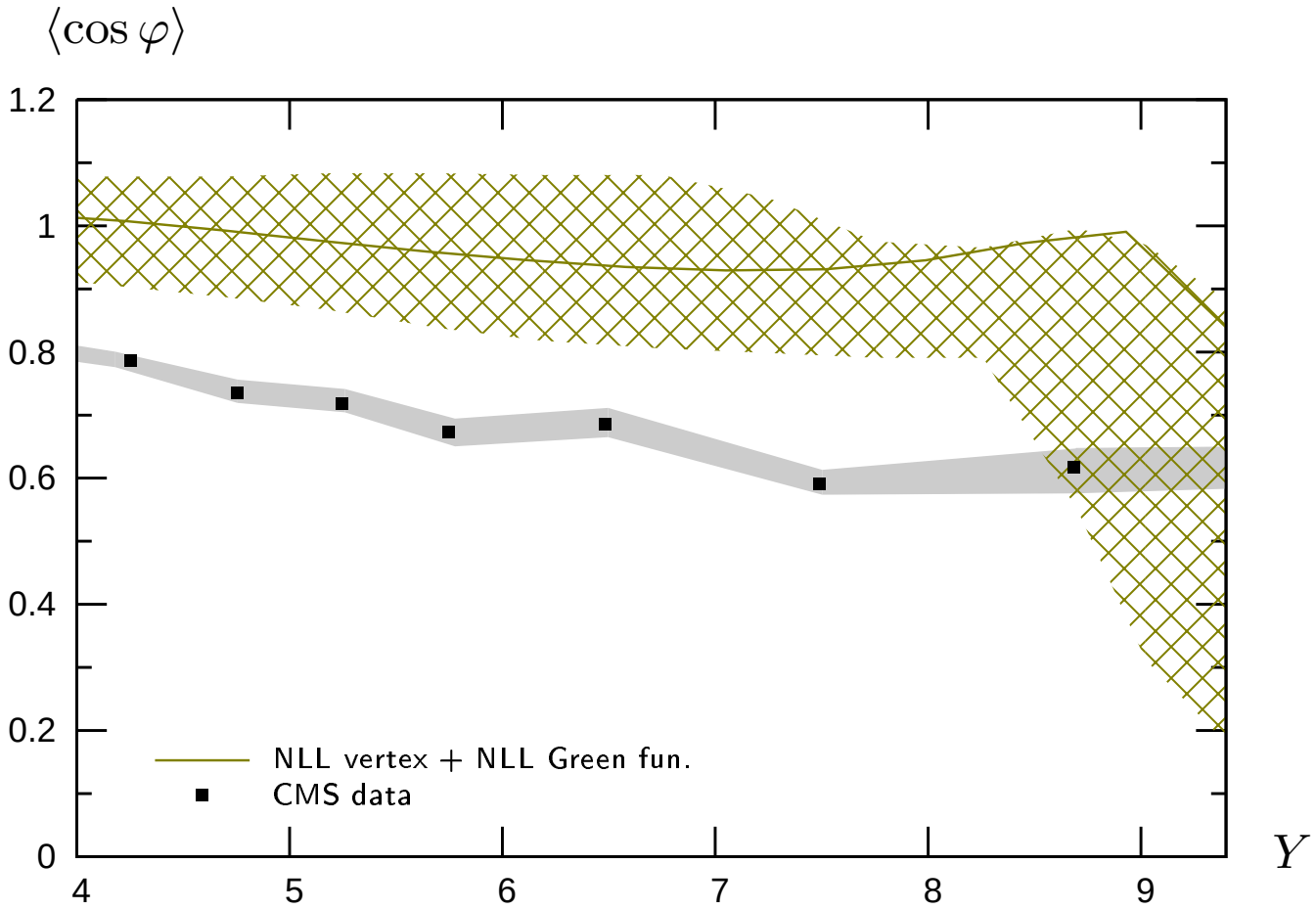

$35\,\mathrm{GeV} < |\mathbf{k}_{J1}| < 60\,\mathrm{GeV}$

$35\,\mathrm{GeV} < |\mathbf{k}_{J2}| < 60\,\mathrm{GeV}$

$0 < y_1 < 4.7$

$0 < y_2 < 4.7$

- None of the BFKL computations describe the data very well
- The result at NLL is still rather dependent on the choice of s_0 and $\mu_R = \mu_F$

Relative variation of $\langle \cos\varphi \rangle$ when using other PDF sets than MSTW 2008

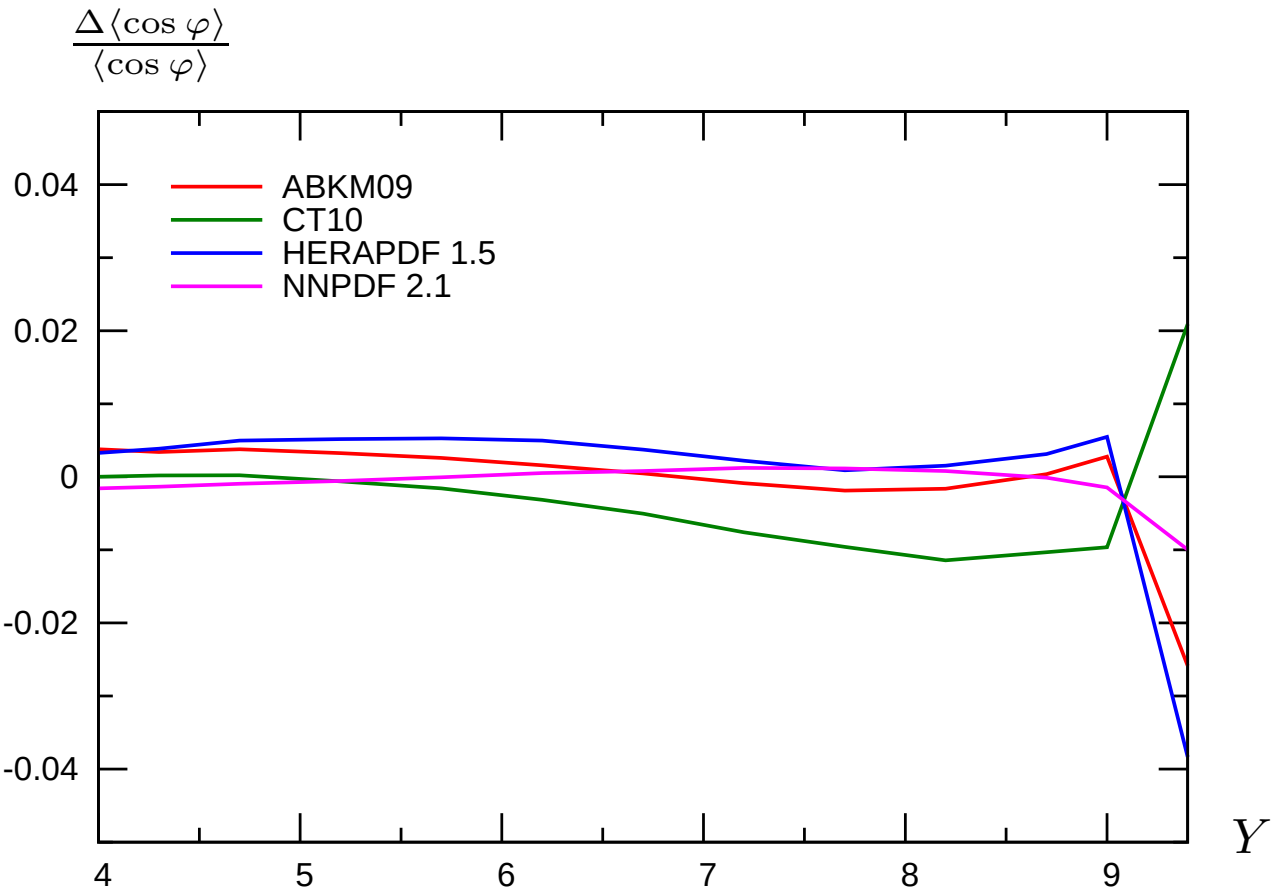

$35\,\mathrm{GeV} < |\mathbf{k}_{J1}| < 60\,\mathrm{GeV}$

$35\,\mathrm{GeV} < |\mathbf{k}_{J2}| < 60\,\mathrm{GeV}$

$0 < y_1 < 4.7$

$0 < y_2 < 4.7$

- The result at NLL is still rather dependent on the choice of s_0 and $\mu_R = \mu_F$
- $\langle \cos\varphi \rangle$ does not depend strongly on the PDF set

Azimuthal correlation $\langle \cos 2\varphi \rangle$

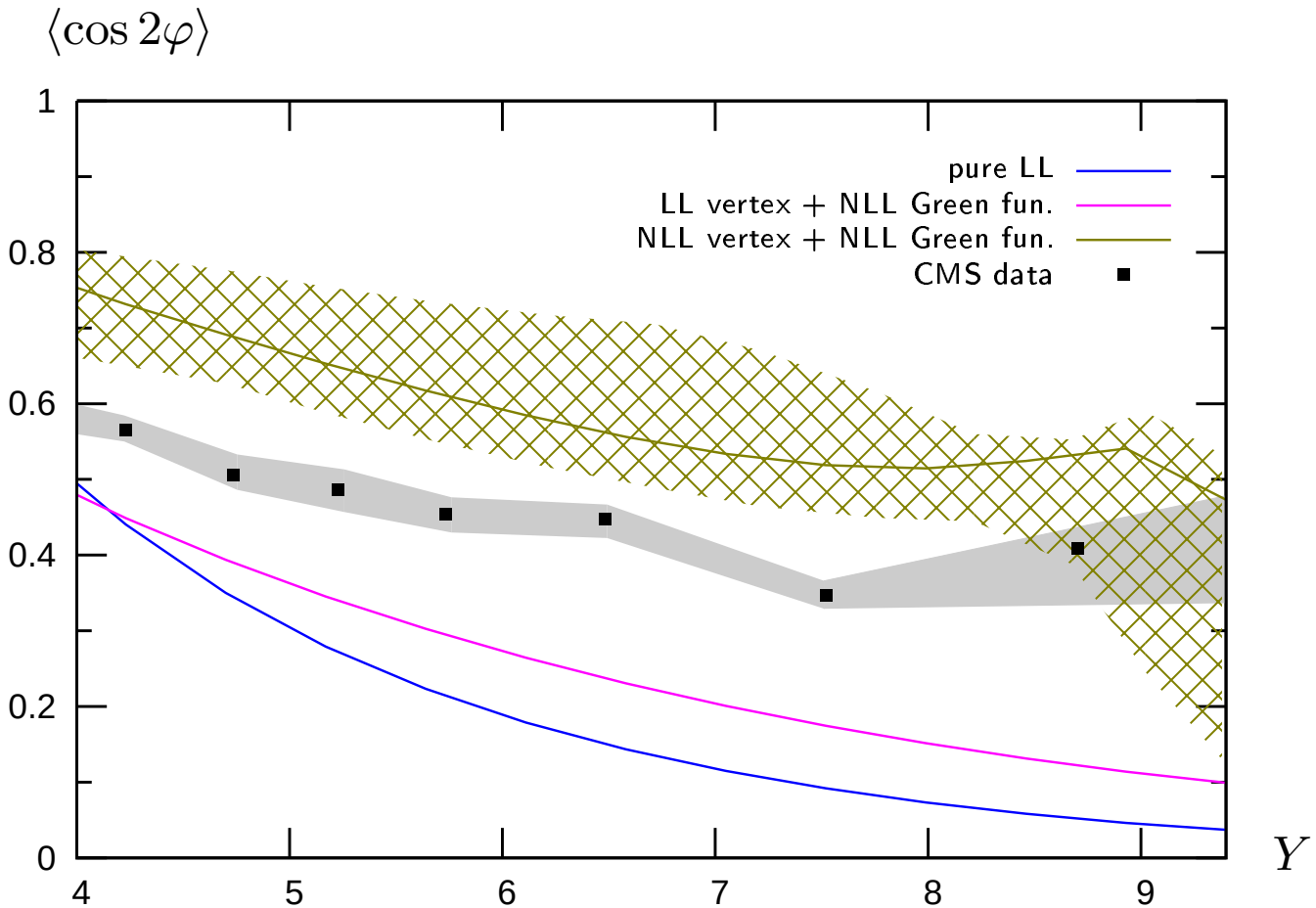

$35\,\mathrm{GeV} < |\mathbf{k}_{J1}| < 60\,\mathrm{GeV}$

$35\,\mathrm{GeV} < |\mathbf{k}_{J2}| < 60\,\mathrm{GeV}$

$0 < y_1 < 4.7$

$0 < y_2 < 4.7$

Azimuthal correlation $\langle \cos 2\varphi \rangle / \langle \cos \varphi \rangle$

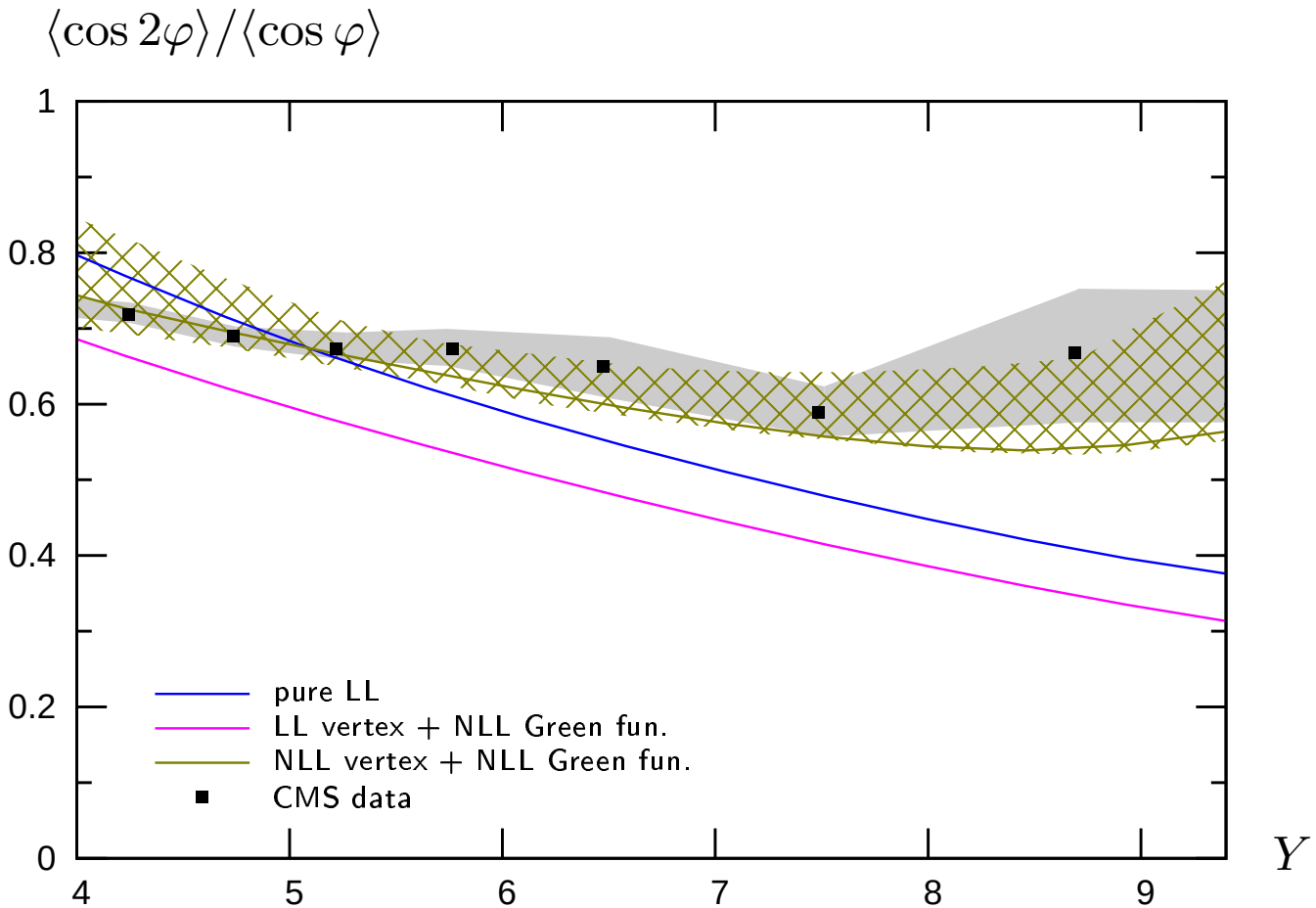

$35\,\mathrm{GeV} < |\mathbf{k}_{J1}| < 60\,\mathrm{GeV}$

$35\,\mathrm{GeV} < |\mathbf{k}_{J2}| < 60\,\mathrm{GeV}$

$0 < y_1 < 4.7$

$0 < y_2 < 4.7$

The observable $\langle \cos 2\varphi \rangle / \langle \cos \varphi \rangle$ is described reasonably well by NLL BFKL and is more stable with respect to the scales

Azimuthal correlation $\langle \cos 2\varphi \rangle / \langle \cos \varphi \rangle$: fixed order NLO versus NLL BFKL

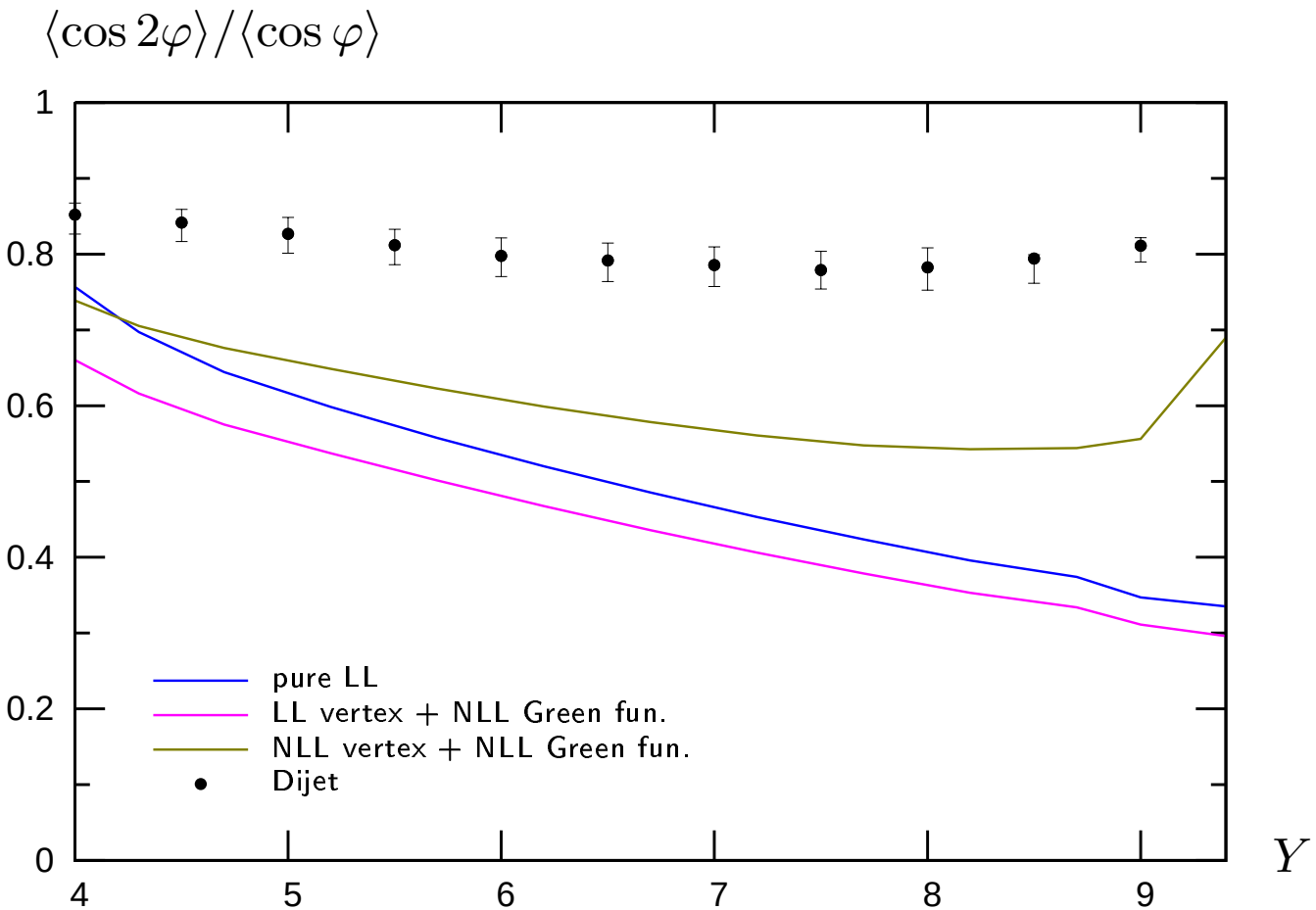

$35\,\mathrm{GeV} < |\mathbf{k}_{J1}| < 60\,\mathrm{GeV}$

$50\,\mathrm{GeV} < |\mathbf{k}_{J2}| < 60\,\mathrm{GeV}$

(such an asymmetric configuration is required to get stable results in a fixed order calculation)

$0 < y_1 < 4.7$
$0 < y_2 < 4.7$

dots: based on the fixed order NLO parton generator *Dijet* (thanks to M. Fontannaz)

- fixed order NLO and NLL BFKL differ significantly for $4.5 < Y < 8$

Results: asymmetric configuration

Azimuthal correlation $\langle \cos 2\varphi \rangle / \langle \cos \varphi \rangle$: fixed order NLO versus NLL BFKL

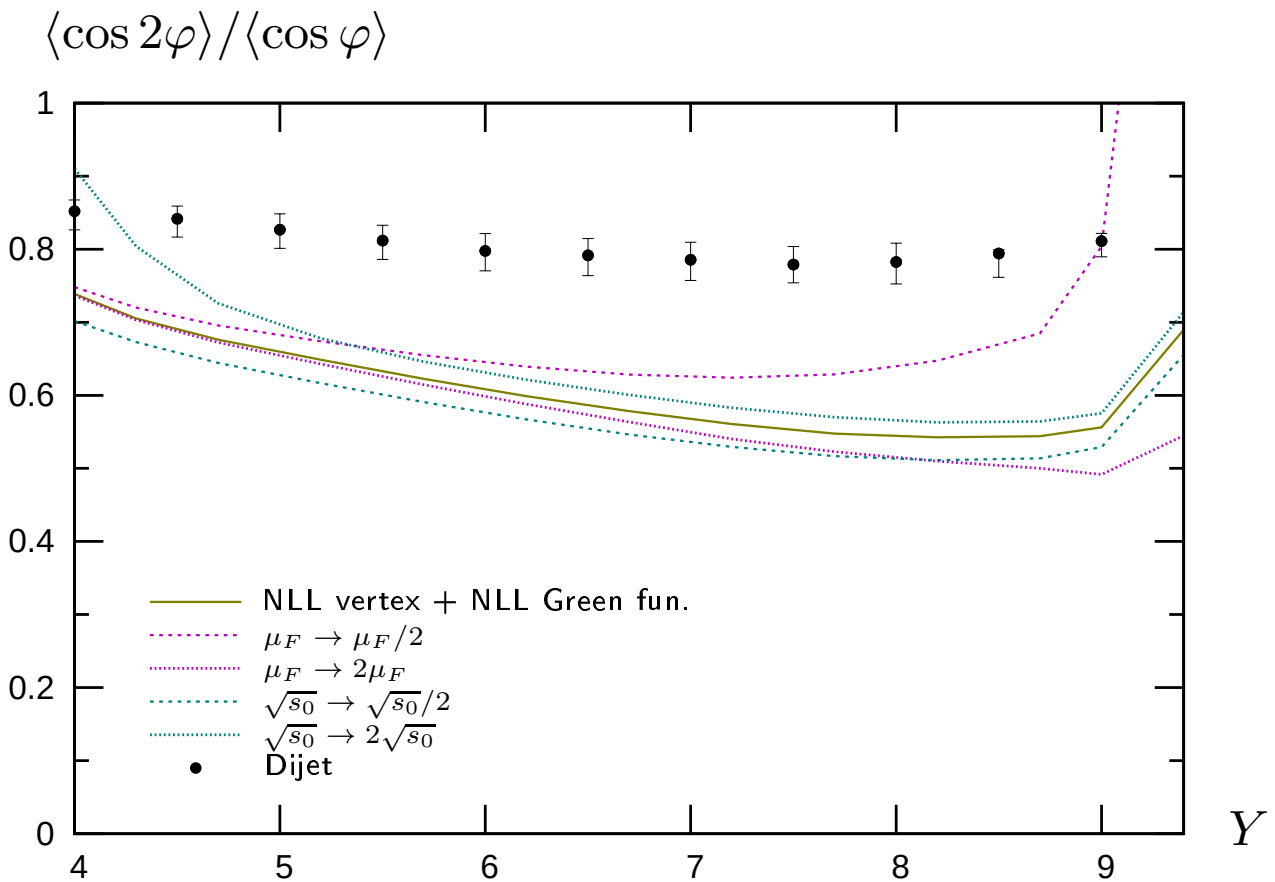

$35\,\mathrm{GeV} < |\mathbf{k}_{J1}| < 60\,\mathrm{GeV}$

$50\,\mathrm{GeV} < |\mathbf{k}_{J2}| < 60\,\mathrm{GeV}$

$0 < y_1 < 4.7$

$0 < y_2 < 4.7$

- fixed order NLO and NLL BFKL differ significantly for $4.5 < Y < 8$
- This result is rather stable w.r.t s_0 and μ choices.

Conclusion

- The effect of NLL corrections to the vertices is very important, similar to the NLL Green's function corrections
- Surprisingly small decorrelation effect
- First comparison to data taken at LHC for the azimuthal correlations
- The quantities $\langle \cos n\varphi \rangle$ are still rather dependent on the choice of the scales
- For the observable $\langle \cos 2\varphi \rangle / \langle \cos \varphi \rangle$:
  - NLL BFKL predictions are more stable with respect to the choice of the scales
  - data is quite well described by NLL BFKL in a symmetric configuration
  - there is a clear difference between fixed-order NLO and our NLL BFKL calculation in an asymmetric configuration

  $\Rightarrow$ It could be interesting to study experimentally this observable also in the asymmetric case

Backup

Results: asymmetric configuration

Azimuthal correlation $\langle \cos\varphi \rangle$: fixed order NLO versus NLL BFKL

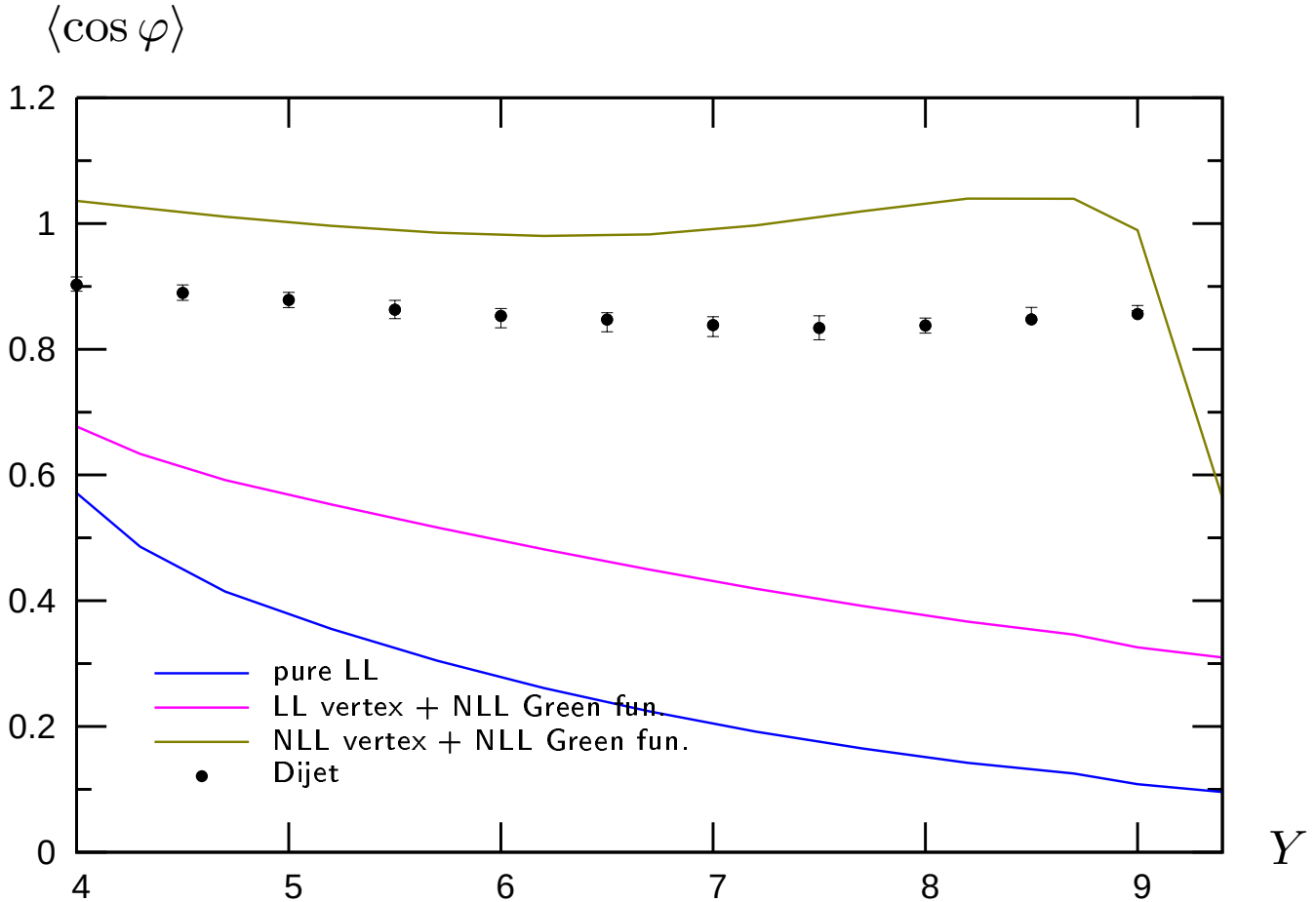

$35\,\mathrm{GeV} < |\mathbf{k}_{J1}| < 60\,\mathrm{GeV}$

$50\,\mathrm{GeV} < |\mathbf{k}_{J2}| < 60\,\mathrm{GeV}$

$0 < y_1 < 4.7$

$0 < y_2 < 4.7$

dots = based on the fixed order NLO parton generator *Dijet* (thanks to M. Fontannaz)

Results: asymmetric configuration

Azimuthal correlation: $\langle \cos\varphi \rangle$

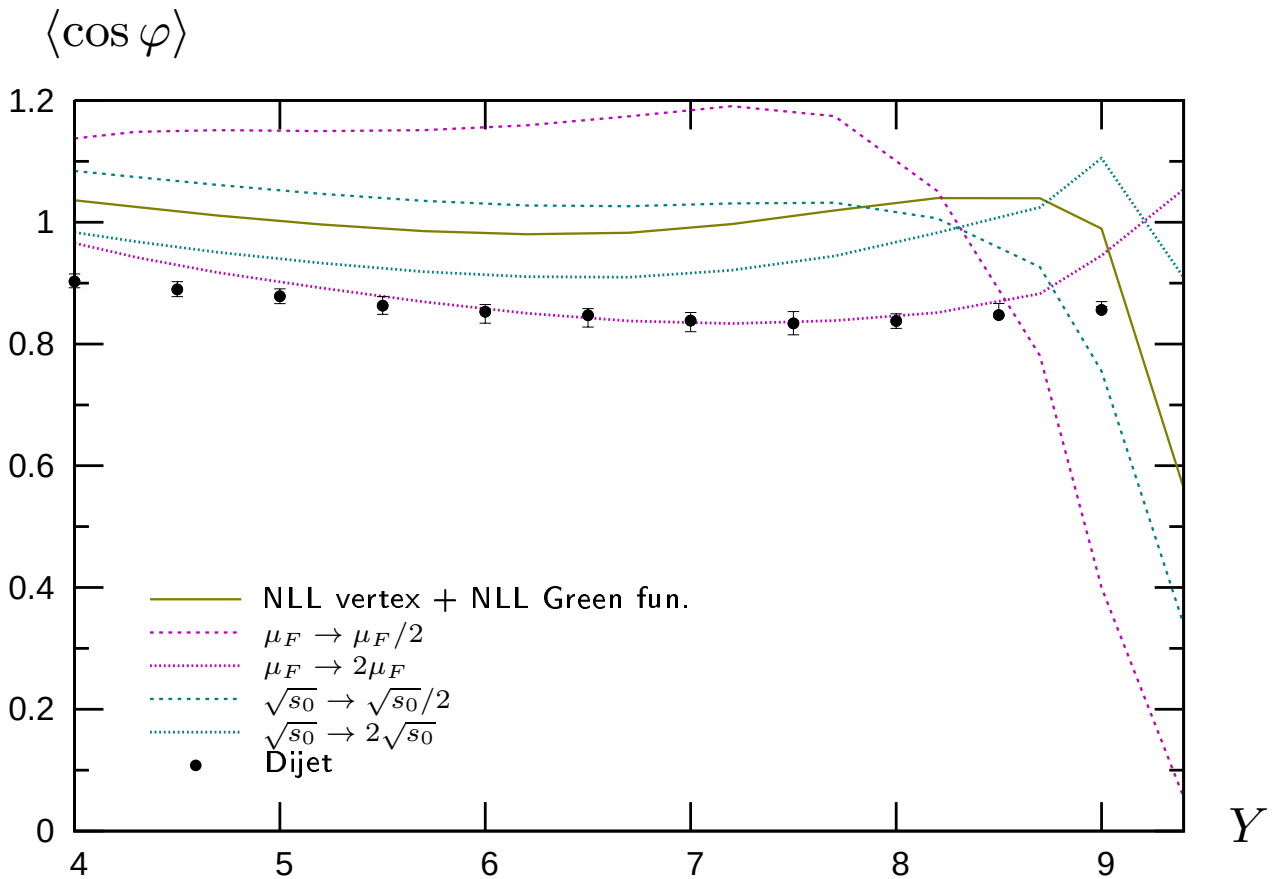

$35\,\mathrm{GeV} < |\mathbf{k}_{J1}| < 60\,\mathrm{GeV}$

$50\,\mathrm{GeV} < |\mathbf{k}_{J2}| < 60\,\mathrm{GeV}$

$0 < y_1 < 4.7$

$0 < y_2 < 4.7$

- Putting (almost) the same scale, exactly the same cuts, we get a difference between fixed order NLO and NLL BFKL for $4.5 < Y < 8.5$
- This difference is washed-out because of s_0 and μ dependency

Azimuthal correlation $\langle \cos 3\varphi \rangle$

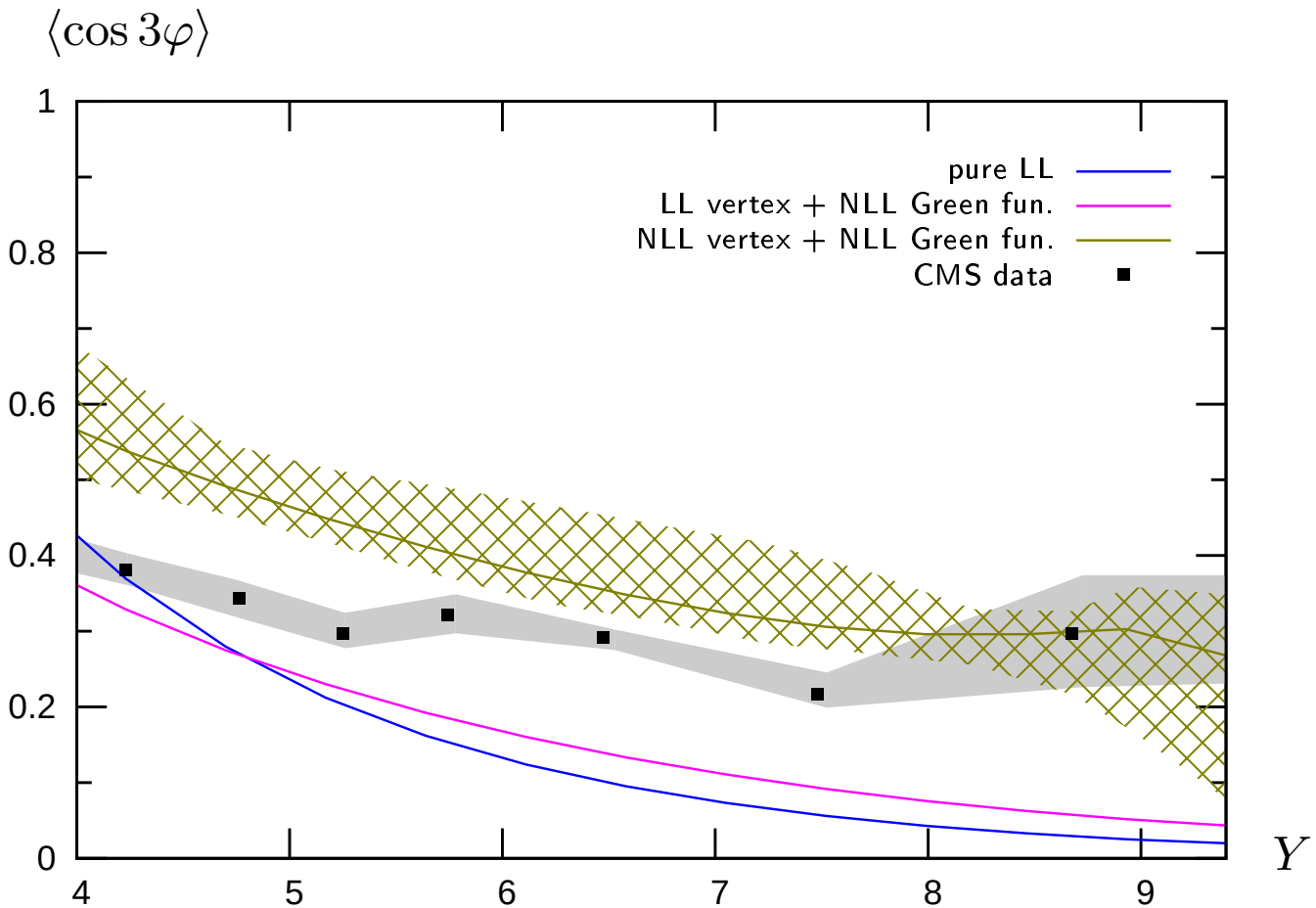

$35\,\mathrm{GeV} < |\mathbf{k}_{J1}| < 60\,\mathrm{GeV}$

$35\,\mathrm{GeV} < |\mathbf{k}_{J2}| < 60\,\mathrm{GeV}$

$0 < y_1 < 4.7$

$0 < y_2 < 4.7$

Taking into account the uncertainty associated with the choice of the scales, NLL BFKL is quite close to the data for $Y \gtrsim 6$.

Azimuthal correlation $\langle \cos 3\varphi \rangle / \langle \cos 2\varphi \rangle$

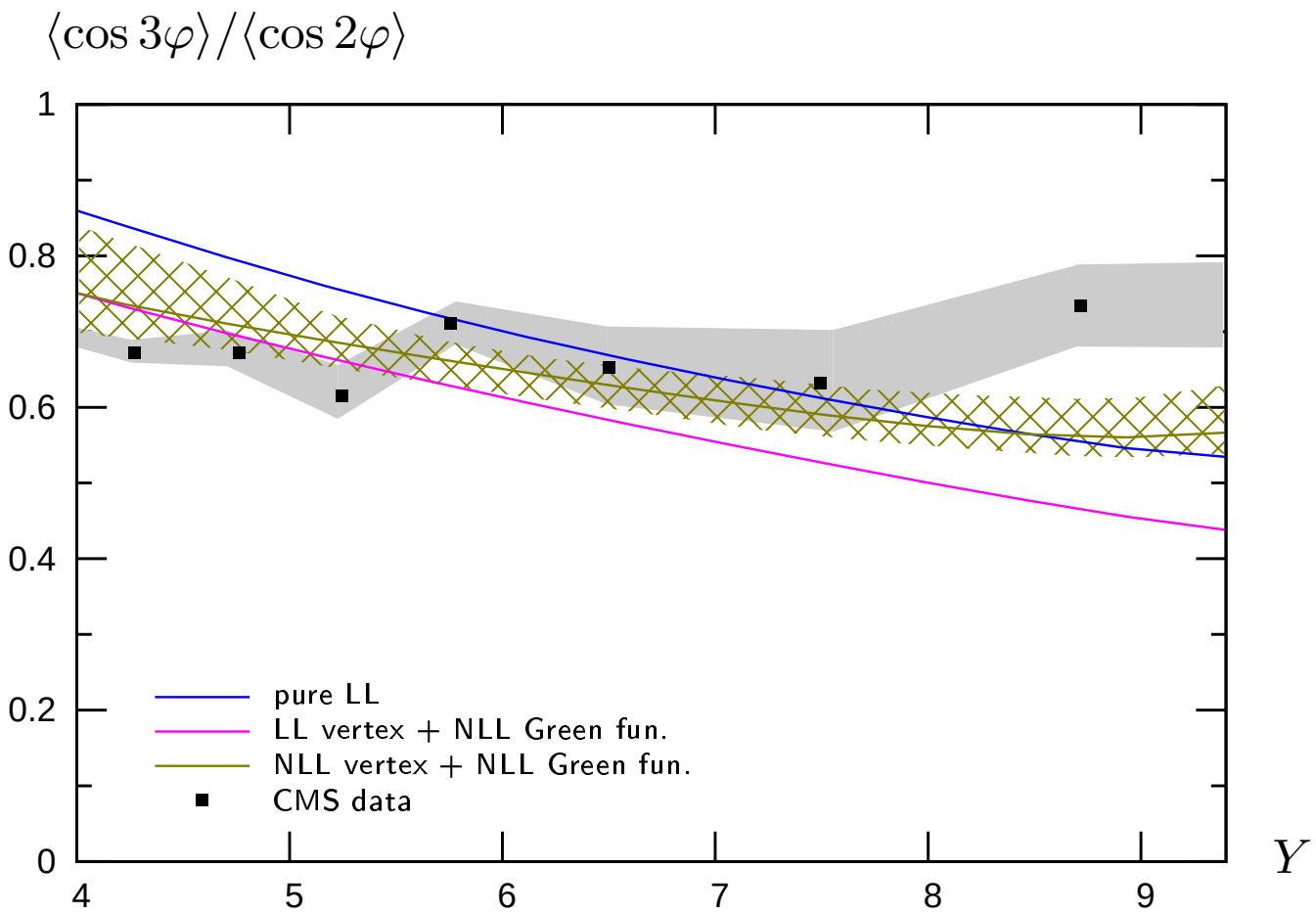

$35\,\mathrm{GeV} < |\mathbf{k}_{J1}| < 60\,\mathrm{GeV}$

$35\,\mathrm{GeV} < |\mathbf{k}_{J2}| < 60\,\mathrm{GeV}$

$0 < y_1 < 4.7$

$0 < y_2 < 4.7$

The 3 different BFKL computations for $\langle \cos 3\varphi \rangle / \langle \cos 2\varphi \rangle$ are quite close to each other

Azimuthal distribution

Computing $\langle \cos(n\phi) \rangle$ up to large values of n gives access to the angular distribution

$$\frac{1}{\sigma}\frac{d\sigma}{d\phi} = \frac{1}{2\pi}\left\{1 + 2\sum_{n=1}^{\infty} \cos(n\phi)\,\langle \cos(n\phi) \rangle\right\}$$

This is a quantity accessible at experiments like ATLAS and CMS

Results: symmetric configuration

Azimuthal distribution

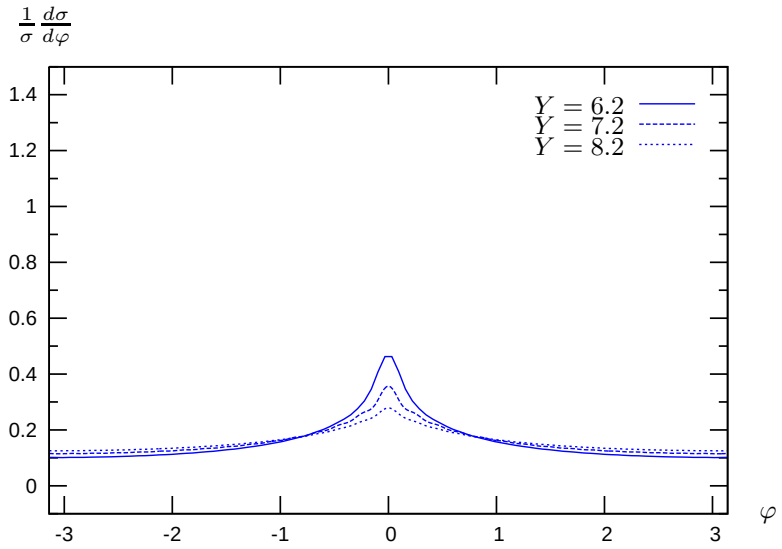

pure LL

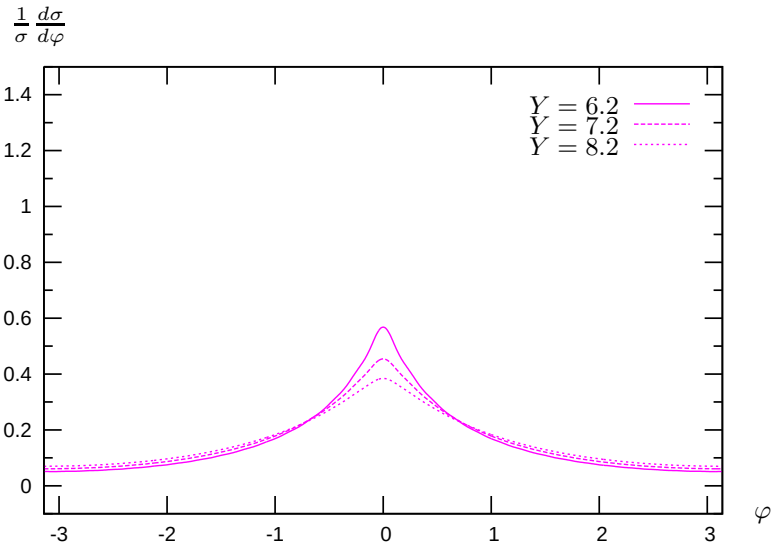

LL vertices + NLL Green's fun.

$$35\,\mathrm{GeV} < |\mathbf{k}_{J1}| < 60\,\mathrm{GeV}$$
$$35\,\mathrm{GeV} < |\mathbf{k}_{J2}| < 60\,\mathrm{GeV}$$

$$0 < y_1 < 4.7$$
$$0 < y_2 < 4.7$$

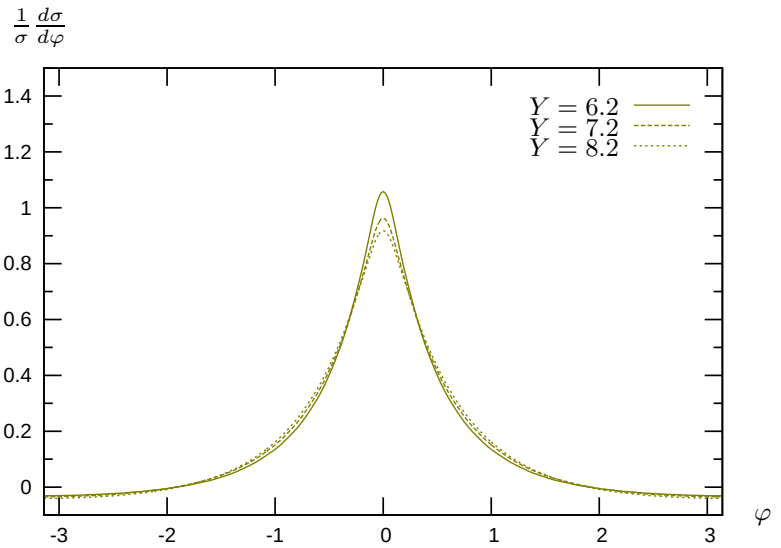

NLL vert. + NLL Green's fun.

Results: symmetric configuration

Azimuthal distribution: stability with respect to s_0 and $\mu_R = \mu_F$

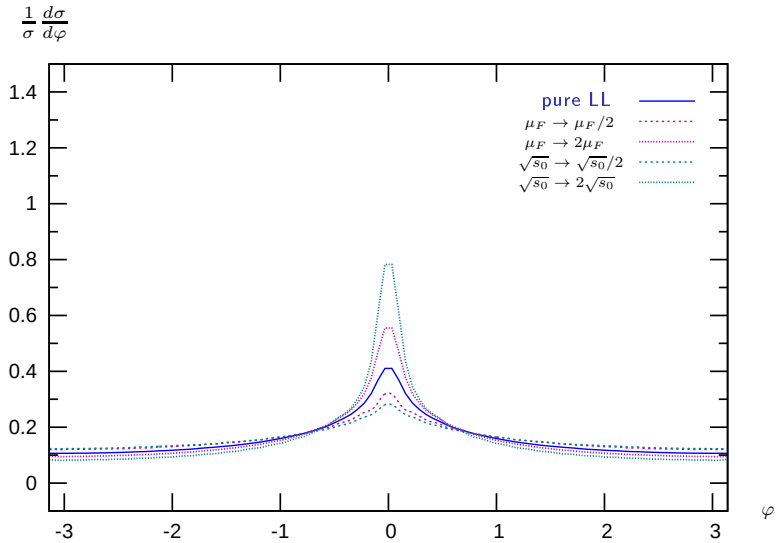

pure LL

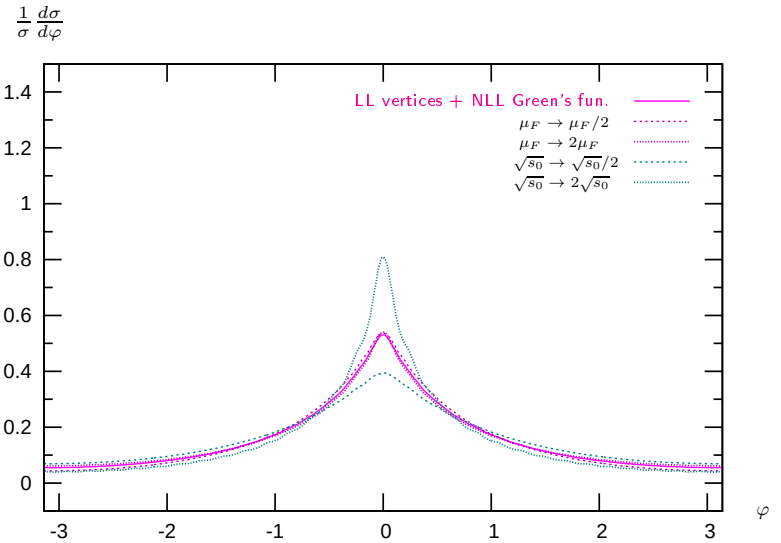

LL vertices + NLL Green's fun.

$$35\,\text{GeV} < |\mathbf{k}_{J1}| < 60\,\text{GeV}$$
$$35\,\text{GeV} < |\mathbf{k}_{J2}| < 60\,\text{GeV}$$

$$0 < y_1 < 4.7$$
$$0 < y_2 < 4.7$$

integrating on the bin:
$6 < Y = y_1 + y_2 < 9.4$

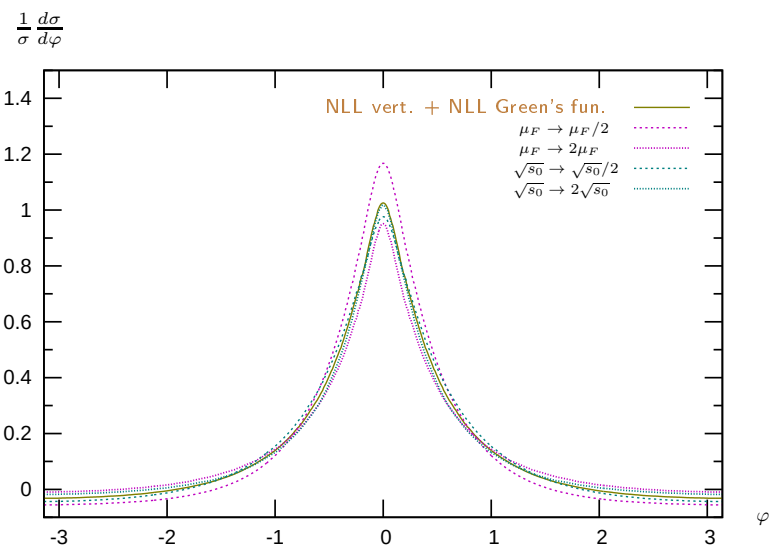

NLL vert. + NLL Green's fun.

Opening the boxes: Impact representation $\gamma^*\,\gamma^* \to \gamma^*\,\gamma^*$ as an example

- Sudakov decomposition: $k_i = \alpha_i\, p_1 + \beta_i\, p_2 + k_{\perp i}$ $\quad (p_1^2 = p_2^2 = 0,\ 2p_1 \cdot p_2 = s)$
- write $\qquad d^4k_i = \frac{s}{2}\, d\alpha_i\, d\beta_i\, d^2k_{\perp i} \qquad \left(\underline{k} = \text{Eucl.} \leftrightarrow k_\perp = \text{Mink.}\right)$
- $t-$channel gluons have non-sense polarizations at large s: $\epsilon_{NS}^{up/down} = \frac{2}{s}\, p_{2/1}$

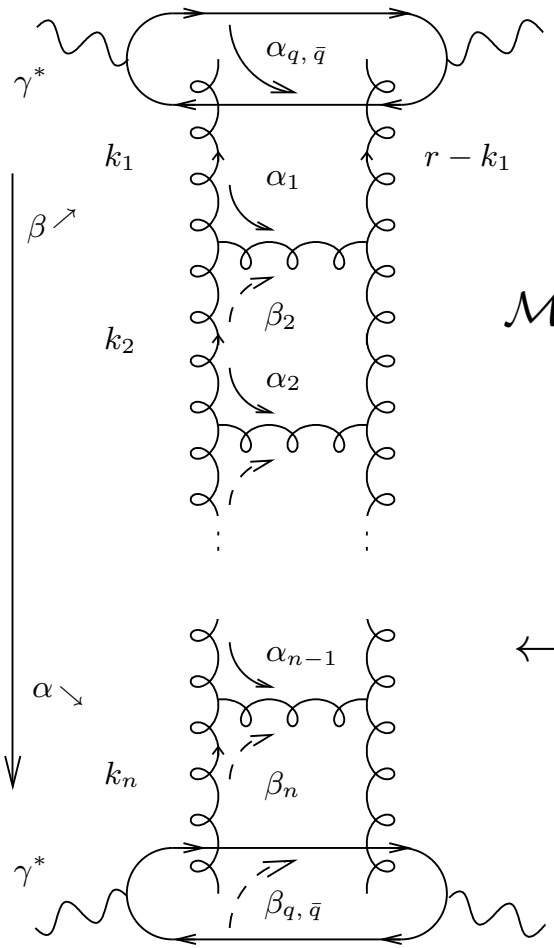

$\Rightarrow$ set $\alpha_1 = 0$ and $\int d\beta_1$ $\Rightarrow$ $\Phi^{\gamma^*\to\gamma^*}(\underline{k}_1, \underline{r} - \underline{k}_1)$
impact factor

$$\mathcal{M} = \frac{is}{(2\pi)^2}\int \frac{d^2\underline{k}}{\underline{k}^2}\, \Phi^{up}(\underline{k},\, \underline{r}-\underline{k}) \int \frac{d^2\underline{k}'}{\underline{k}'^2}\, \Phi^{down}(-\underline{k}',\, -\underline{r}+\underline{k}') \times \int_{\delta-i\infty}^{\delta+i\infty} \frac{d\omega}{2\pi i} \left(\frac{s}{s_0}\right)^{\omega} G_\omega(\underline{k}, \underline{k}', \underline{r})$$

$\longleftarrow$ multi-Regge kinematics

$\Rightarrow$ set $\beta_n = 0$ and $\int d\alpha_n$ $\Rightarrow$ $\Phi^{\gamma^*\to\gamma^*}(-\underline{k}_n, -\underline{r} + \underline{k}_n)$

Angular coefficients

$$\mathcal{C}_m \equiv \int \mathrm{d}\phi_{J1}\,\mathrm{d}\phi_{J2}\,\cos\left(m(\phi_{J,1}-\phi_{J,2}-\pi)\right)$$
$$\times \int \mathrm{d}^2\mathbf{k}_1\,\mathrm{d}^2\mathbf{k}_2\,\Phi(\mathbf{k}_{J1},x_{J,1},-\mathbf{k}_1)\,G(\mathbf{k}_1,\mathbf{k}_2,\hat{s})\,\Phi(\mathbf{k}_{J2},x_{J,2},\mathbf{k}_2).$$

- $m=0 \implies$ cross-section

$$\frac{\mathrm{d}\sigma}{\mathrm{d}|\mathbf{k}_{J1}|\,\mathrm{d}|\mathbf{k}_{J2}|\,\mathrm{d}y_{J1}\,\mathrm{d}y_{J2}} = \mathcal{C}_0$$

- $m>0 \implies$ azimuthal decorrelation

$$\langle\cos(m\phi)\rangle \equiv \langle\cos\left(m(\phi_{J,1}-\phi_{J,2}-\pi)\right)\rangle = \frac{\mathcal{C}_m}{\mathcal{C}_0}$$

Jet algorithms

- a jet algorithm should be IR safe, both for soft and collinear singularities
- the most common jet algorithm are:
  - k_t algorithms (IR safe but time consuming for multiple jets configurations)
  - cone algorithm (not IR safe in general; can be made IR safe at NLO: Ellis, Kunszt, Soper)

Cone jet algorithm at NLO (Ellis, Kunszt, Soper)

- Should partons $(|\mathbf{p}_1|, \phi_1, y_1)$ and $(\mathbf{p}_2|, \phi_2, y_2)$ be combined in a single jet? $|\mathbf{p}_i|$ =transverse energy deposit in the calorimeter cell i of parameter $\Omega = (y_i, \phi_i)$ in $y - \phi$ plane
- define transverse energy of the jet: $p_J = |\mathbf{p}_1| + |\mathbf{p}_2|$
- jet axis:

$$\Omega_c \begin{cases} y_J = \dfrac{|\mathbf{p}_1|\, y_1 + |\mathbf{p}_2|\, y_2}{p_J} \\ \phi_J = \dfrac{|\mathbf{p}_1|\, \phi_1 + |\mathbf{p}_2|\, \phi_2}{p_J} \end{cases}$$

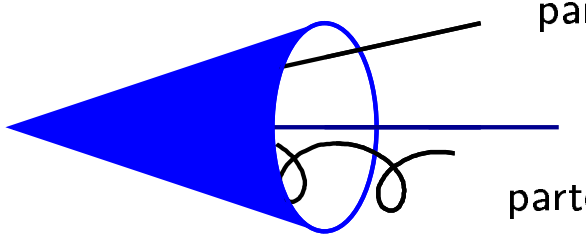

$\Omega = (y_i, \phi_i)$ in $y - \phi$ plane

If distances $|\Omega_i - \Omega_c|^2 \equiv (y_i - y_c)^2 + (\phi_i - \phi_c)^2 < R^2$ $(i = 1$ and $i = 2)$

$\Longrightarrow$ partons 1 and 2 are in the same cone Ω_c

combined condition: $|\Omega_1 - \Omega_2| < \dfrac{|\mathbf{p}_1| + |\mathbf{p}_2|}{max(|\mathbf{p}_1|, |\mathbf{p}_2|)} R$

LL jet vertex and cone algorithm

$\mathbf{k}, \mathbf{k}'$ = Euclidian two dimensional vectors

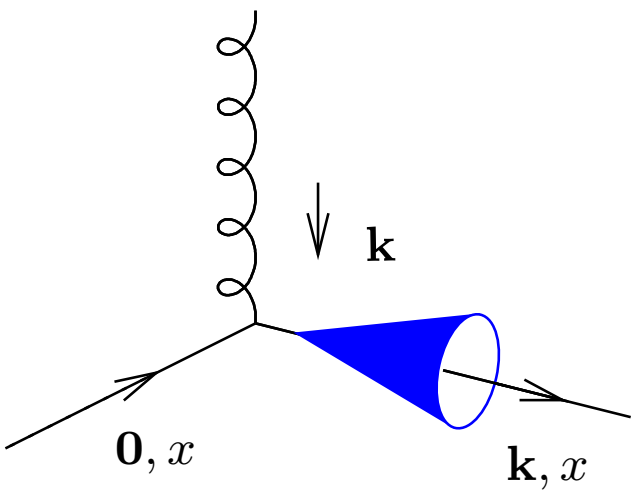

$$\mathcal{S}_J^{(2)}(k_\perp; x) = \delta\left(1 - \frac{x_J}{x}\right) |\mathbf{k}|\, \delta^{(2)}(\mathbf{k} - \mathbf{k}_J)$$

NLL jet vertex and cone algorithm

$\mathbf{k}, \mathbf{k}'$ = Euclidian two dimensional vectors

$$\mathcal{S}_J^{(3,\text{cone})}(\mathbf{k}', \mathbf{k}-\mathbf{k}', xz; x) =$$

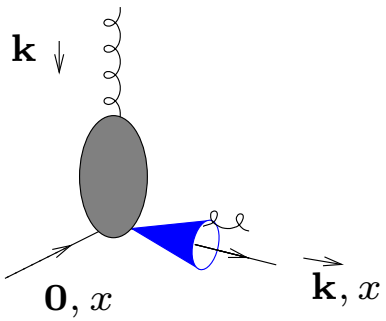

$$\mathcal{S}_J^{(2)}(\mathbf{k}, x)\,\Theta\left(\left[\frac{|\mathbf{k}-\mathbf{k}'|+|\mathbf{k}'|}{\max(|\mathbf{k}-\mathbf{k}'|,|\mathbf{k}'|)}R_{\text{cone}}\right]^2 - \left[\Delta y^2+\Delta\phi^2\right]\right)$$

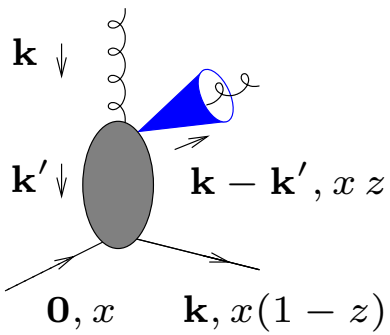

$$+\,\mathcal{S}_J^{(2)}(\mathbf{k}-\mathbf{k}', xz)\,\Theta\left(\left[\Delta y^2+\Delta\phi^2\right] - \left[\frac{|\mathbf{k}-\mathbf{k}'|+|\mathbf{k}'|}{\max(|\mathbf{k}-\mathbf{k}'|,|\mathbf{k}'|)}R_{\text{cone}}\right]^2\right)$$

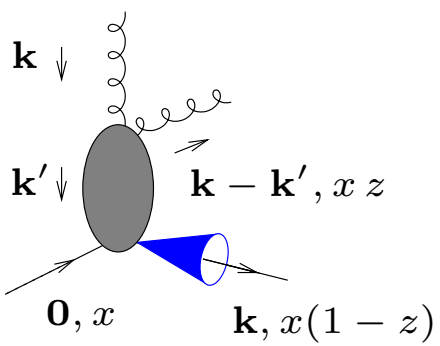

$$+\,\mathcal{S}_J^{(2)}(\mathbf{k}', x(1-z))\,\Theta\left(\left[\Delta y^2+\Delta\phi^2\right] - \left[\frac{|\mathbf{k}-\mathbf{k}'|+|\mathbf{k}'|}{\max(|\mathbf{k}-\mathbf{k}'|,|\mathbf{k}'|)}R_{\text{cone}}\right]^2\right),$$

The LL impact factor

$$V_{\rm a}^{(0)}(\mathbf{k},x) = h_{\rm a}^{(0)}(\mathbf{k})\mathcal{S}_J^{(2)}(\mathbf{k};x)$$

with: $$h_{\rm a}^{(0)}(\mathbf{k}) = \frac{\alpha_s}{\sqrt{2}}\frac{C_{A/F}}{\mathbf{k}^2}\,,$$

$$\mathcal{S}_J^{(2)}(\mathbf{k};x) = \delta\left(1-\frac{x_J}{x}\right)|\mathbf{k}_J|\delta^{(2)}(\mathbf{k}-\mathbf{k}_J)$$

NLL corrections to the jet vertex: the quark part (Bartels, Colferai, Vacca)

$$
\begin{aligned}
V_{\mathrm{q}}^{(1)}(\mathbf{k},x) = &\left[\left(\frac{3}{2}\ln\frac{\mathbf{k}^2}{\Lambda^2}-\frac{15}{4}\right)\frac{C_F}{\pi}+\left(\frac{85}{36}+\frac{\pi^2}{4}\right)\frac{C_A}{\pi}-\frac{5}{18}\frac{N_f}{\pi}-b_0\ln\frac{\mathbf{k}^2}{\mu^2}\right]V_{\mathrm{q}}^{(0)}(\mathbf{k},x)\\
&+\int \mathrm{d}z\left(\frac{C_F}{\pi}\frac{1-z}{2}+\frac{C_A}{\pi}\frac{z}{2}\right)V_{\mathrm{q}}^{(0)}(\mathbf{k},xz)\\
&+\frac{C_A}{\pi}\int\frac{\mathrm{d}^2\mathbf{k}'}{\pi}\int\mathrm{d}z\left[\frac{1+(1-z)^2}{2z}\left((1-z)\frac{(\mathbf{k}-\mathbf{k}')\cdot((1-z)\mathbf{k}-\mathbf{k}')}{(\mathbf{k}-\mathbf{k}')^2((1-z)\mathbf{k}-\mathbf{k}')^2}h_{\mathrm{q}}^{(0)}(\mathbf{k}')\mathcal{S}_J^{(3)}(\mathbf{k}',\mathbf{k}-\mathbf{k}',xz;x)\right.\right.\\
&\qquad\left.-\frac{1}{\mathbf{k}'^2}\Theta(\Lambda^2-\mathbf{k}'^2)V_{\mathrm{q}}^{(0)}(\mathbf{k},xz)\right)\\
&\qquad\left.-\frac{1}{z(\mathbf{k}-\mathbf{k}')^2}\Theta(|\mathbf{k}-\mathbf{k}'|-z(|\mathbf{k}-\mathbf{k}'|+|\mathbf{k}'|))V_{\mathrm{q}}^{(0)}(\mathbf{k}',x)\right]\\
&+\frac{C_F}{2\pi}\int\mathrm{d}z\,\frac{1+z^2}{1-z}\int\frac{\mathrm{d}^2\mathbf{l}}{\pi\mathbf{l}^2}\left[\frac{\mathcal{N}C_F}{\mathbf{l}^2+(\mathbf{l}-\mathbf{k})^2}\left(\mathcal{S}_J^{(3)}(z\mathbf{k}+(1-z)\mathbf{l},(1-z)(\mathbf{k}-\mathbf{l}),x(1-z);x)\right.\right.\\
&\qquad\left.+\mathcal{S}_J^{(3)}(\mathbf{k}-(1-z)\mathbf{l},(1-z)\mathbf{l},x(1-z);x)\right)\\
&\qquad\left.-\Theta\left(\frac{\Lambda^2}{(1-z)^2}-\mathbf{l}^2\right)\left(V_{\mathrm{q}}^{(0)}(\mathbf{k},x)+V_{\mathrm{q}}^{(0)}(\mathbf{k},xz)\right)\right]\\
&-\frac{2C_F}{\pi}\int\mathrm{d}z\left(\frac{1}{1-z}\right)\int\frac{\mathrm{d}^2\mathbf{l}}{\pi\mathbf{l}^2}\left[\frac{\mathcal{N}C_F}{\mathbf{l}^2+(\mathbf{l}-\mathbf{k})^2}S_J^{(2)}(\mathbf{k},x)-\Theta\left(\frac{\Lambda^2}{(1-z)^2}-\mathbf{l}^2\right)V_{\mathrm{q}}^{(0)}(\mathbf{k},x)\right]
\end{aligned}
$$

NLL corrections to the jet vertex: the gluon part (Bartels, Colferai, Vacca)

$$
\begin{aligned}
V_{\mathrm{g}}^{(1)}(\mathbf{k},x) = &\left[\left(\frac{11}{6}\frac{C_A}{\pi}-\frac{1}{3}\frac{N_f}{\pi}\right)\ln\frac{\mathbf{k}^2}{\Lambda^2}+\left(\frac{\pi^2}{4}-\frac{67}{36}\right)\frac{C_A}{\pi}+\frac{13}{36}\frac{N_f}{\pi}-b_0\ln\frac{\mathbf{k}^2}{\mu^2}\right]V_{\mathrm{g}}^{(0)}(\mathbf{k},x)\\
&+\int \mathrm{d}z\,\frac{N_f}{\pi}\frac{C_F}{C_A}z(1-z)V_{\mathrm{g}}^{(0)}(\mathbf{k},xz)\\
&+\frac{N_f}{\pi}\int\frac{\mathrm{d}^2\mathbf{k}'}{\pi}\int_0^1\mathrm{d}z\,P_{\mathrm{qg}}(z)\left[\frac{h_{\mathrm{q}}^{(0)}(\mathbf{k}')}{(\mathbf{k}-\mathbf{k}')^2+\mathbf{k}'^2}\mathcal{S}_J^{(3)}(\mathbf{k}',\mathbf{k}-\mathbf{k}',xz;x)-\frac{1}{\mathbf{k}'^2}\Theta(\Lambda^2-\mathbf{k}'^2)V_{\mathrm{q}}^{(0)}(\mathbf{k},xz)\right]\\
&+\frac{N_f}{2\pi}\int\frac{\mathrm{d}^2\mathbf{k}'}{\pi}\int_0^1\mathrm{d}z\,P_{\mathrm{qg}}(z)\frac{\mathcal{N}C_A}{((1-z)\mathbf{k}-\mathbf{k}')^2}\left[z(1-z)\frac{(\mathbf{k}-\mathbf{k}')\cdot\mathbf{k}'}{(\mathbf{k}-\mathbf{k}')^2\mathbf{k}'^2}\mathcal{S}_J^{(3)}(\mathbf{k}',\mathbf{k}-\mathbf{k}',xz;x)\right.\\
&\qquad\left.-\frac{1}{\mathbf{k}^2}\Theta\left(\Lambda^2-((1-z)\mathbf{k}-\mathbf{k}')^2\right)\mathcal{S}_J^{(2)}(\mathbf{k},x)\right]\\
&+\frac{C_A}{\pi}\int_0^1\frac{\mathrm{d}z}{1-z}\left[(1-z)P(1-z)\right]\int\frac{\mathrm{d}^2\mathbf{l}}{\pi\mathbf{l}^2}\left\{\frac{\mathcal{N}C_A}{\mathbf{l}^2+(\mathbf{l}-\mathbf{k})^2}\left[\mathcal{S}_J^{(3)}(z\mathbf{k}+(1-z)\mathbf{l},(1-z)(\mathbf{k}-\mathbf{l}),x(1-z);x)\right.\right.\\
&\qquad\left.+\mathcal{S}_J^{(3)}(\mathbf{k}-(1-z)\mathbf{l},(1-z)\mathbf{l},x(1-z);x)\right]\\
&\qquad\left.-\Theta\left(\frac{\Lambda^2}{(1-z)^2}-\mathbf{l}^2\right)\left[V_{\mathrm{g}}^{(0)}(\mathbf{k},x)+V_{\mathrm{g}}^{(0)}(\mathbf{k},xz)\right]\right\}\\
&-\frac{2C_A}{\pi}\int_0^1\frac{\mathrm{d}z}{1-z}\int\frac{\mathrm{d}^2\mathbf{l}}{\pi\mathbf{l}^2}\left[\frac{\mathcal{N}C_A}{\mathbf{l}^2+(\mathbf{l}-\mathbf{k})^2}S_J^{(2)}(\mathbf{k},x)-\Theta\left(\frac{\Lambda^2}{(1-z)^2}-\mathbf{l}^2\right)V_{\mathrm{g}}^{(0)}(\mathbf{k},x)\right]\\
&+\frac{C_A}{\pi}\int\frac{\mathrm{d}^2\mathbf{k}'}{\pi}\int_0^1\mathrm{d}z\left[P(z)\left((1-z)\frac{(\mathbf{k}-\mathbf{k}')\cdot((1-z)\mathbf{k}-\mathbf{k}')}{(\mathbf{k}-\mathbf{k}')^2((1-z)\mathbf{k}-\mathbf{k}')^2}h_{\mathrm{g}}^{(0)}(\mathbf{k}')\right.\right.\\
&\qquad\left.\times\mathcal{S}_J^{(3)}(\mathbf{k}',\mathbf{k}-\mathbf{k}',xz;x)-\frac{1}{\mathbf{k}'^2}\Theta(\Lambda^2-\mathbf{k}'^2)V_{\mathrm{g}}^{(0)}(\mathbf{k},xz)\right)\\
&\qquad\left.-\frac{1}{z(\mathbf{k}-\mathbf{k}')^2}\Theta(|\mathbf{k}-\mathbf{k}'|-z(|\mathbf{k}-\mathbf{k}'|+|\mathbf{k}'|))V_{\mathrm{g}}^{(0)}(\mathbf{k}',x)\right]
\end{aligned}
$$